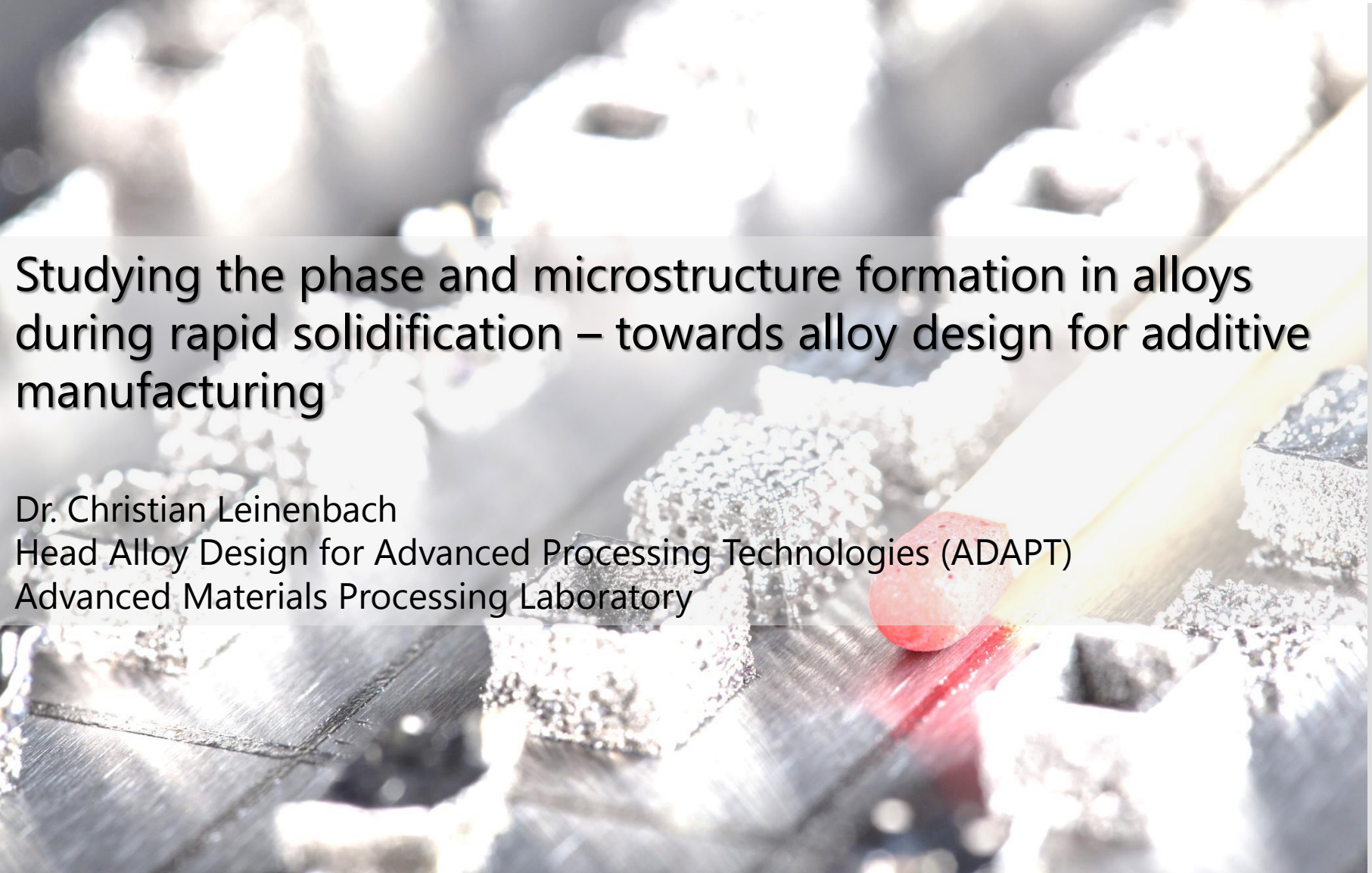


Willkommen  
Welcome  
Bienvenue



# Studying the phase and microstructure formation in alloys during rapid solidification – towards alloy design for additive manufacturing

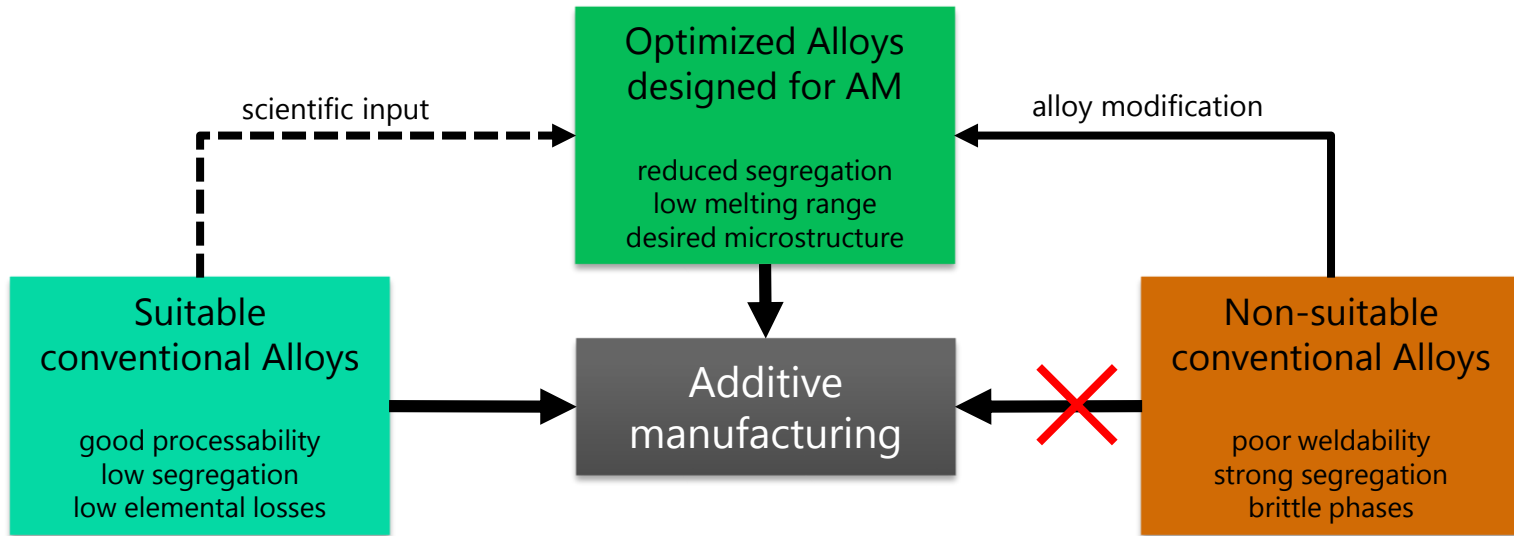
Dr. Christian Leinenbach  
Head Alloy Design for Advanced Processing Technologies (ADAPT)  
Advanced Materials Processing Laboratory

- Materials aspects related to AM – some basics
- Development of an ODS-TiAl alloy for AM
  - Microstructure formation during rapid solidification
  - Microstructure of AM processed ODS-TiAl
- Development of bronze/diamond composites for AM
  - SLM processing of bronze/diamond composites
  - Rapid solidification of Cu-Sn-Ti alloys
- Summary and outlook

- Materials aspects related to AM – some basics
- Development of an ODS-TiAl alloy for AM
  - Microstructure formation during rapid solidification
  - Microstructure of AM processed ODS-TiAl
- Development of bronze/diamond composites for AM
  - SLM processing of bronze/diamond composites
  - Rapid solidification of Cu-Sn-Ti alloys
- Summary and outlook

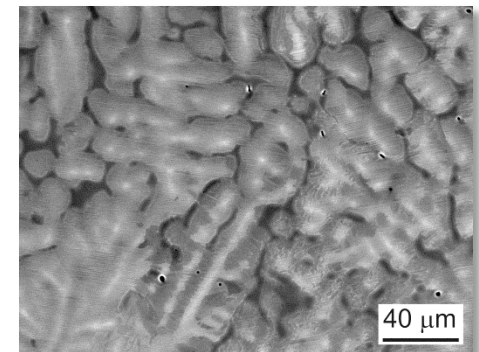
- In Switzerland, there is a specific need for AM of the following materials
  - Advanced high-temperature alloys ( $\gamma'$ -hardening Ni-based alloys, Co-based alloys, TiAl) for power generation and aerospace applications
  - Tool steels, HSS, metal-superabrasives composites for advanced shape forming tools (grinding, cutting, milling etc.)
  - Precious metal alloys (Au-, Pd-, Pt-based) for jewelry and watches
- Useful information on the processability of those materials is very limited or not existing!

# What are the problems with AM processing?

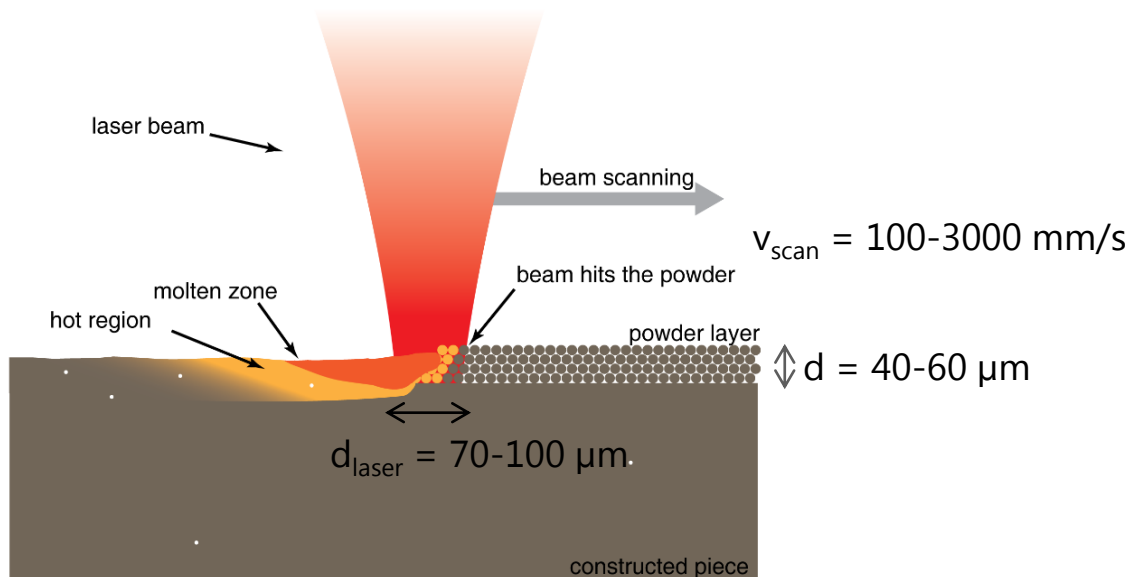


- typical problems in AM with non-suitable alloys:
    - hot cracking
    - strong segregation of specific elements
    - thermal cracking of brittle phases due to high stresses
- } alloy chemistry dependent

- *ex situ* studies on rapid solidified alloys
  - characterization of microstructure, phase analysis and segregation tendency
  - influence of alloying elements on behavior under AM conditions
  - screening of potential / already available / new alloys
- *in situ* studies to follow solidification and transformation



# A look into the AM process conditions



Thermal penetration depth

$$l_{therm} = 2\sqrt{D\tau}$$

$$D = \frac{k}{\rho C_p} \quad \tau = \frac{d_{laser}}{v_{scan}}$$

Example:

$$D_{steel} \approx 4 \text{ mm}^2/\text{s}$$

$$d_{laser} = 0.1 \text{ mm}$$

$$v_{scan} = 1000 \text{ mm/s}$$

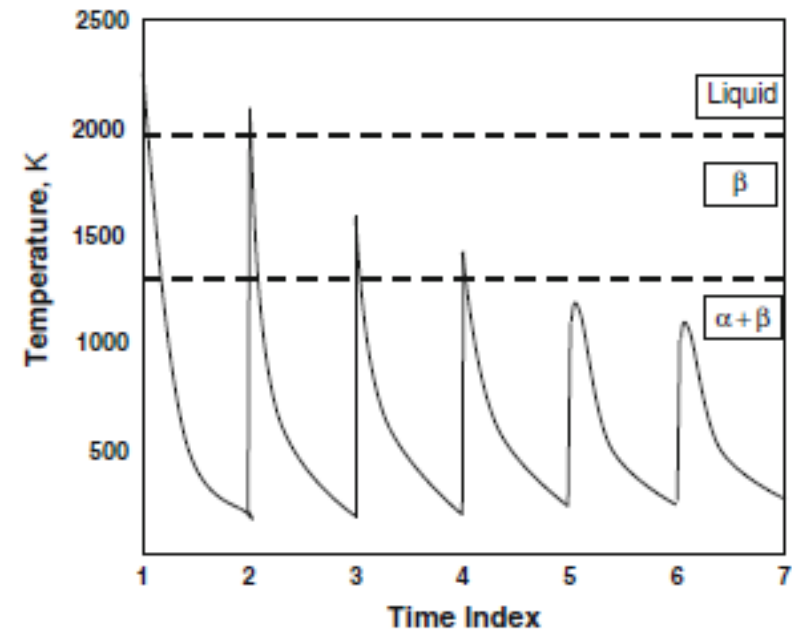
$$\rightarrow l_{therm} = 40 \mu\text{m}$$

- A small material volume is rapidly heated and cooled with large thermal gradients ( $\Delta T \approx 10^3 - 10^4 \text{ K/s}$ )
- The molten material solidifies very rapidly!

# Thermal history during AM

- Characteristics of AM processing
  - Fast heating and cooling ( $\Delta T \approx 10^4$  K/s)
    - suppressed phase transformations; supersaturated phases
    - segregation
    - thermal residual stresses
  - Unidirectional heat flow into building plate/substrate
    - textured grains; anisotropic properties
  - Every layer undergoes repeated heating and cooling cycles; temperatures can exceed  $T_{liq}$  or  $T_{\alpha \leftrightarrow \beta}$ 
    - Multiple phase transformations, complex microstructures with unwanted properties

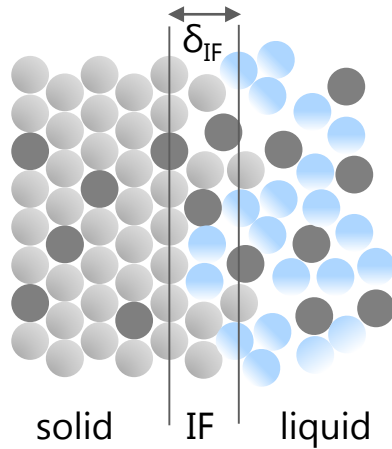
thermal profile of a single layer AM processed Ti-6Al-4V



/W.E. Frazier, J. Mater. Eng. Perform. 23 (2014) 1917/

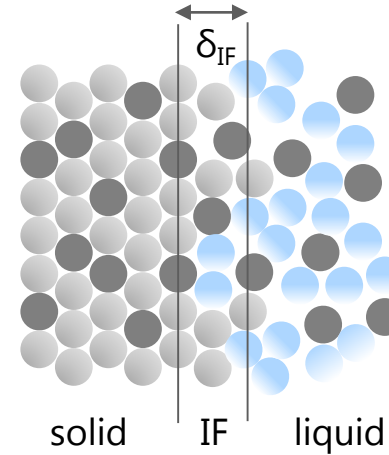
# Solid-liquid interface: slow vs. rapid cooling

slow (equilibrium) cooling

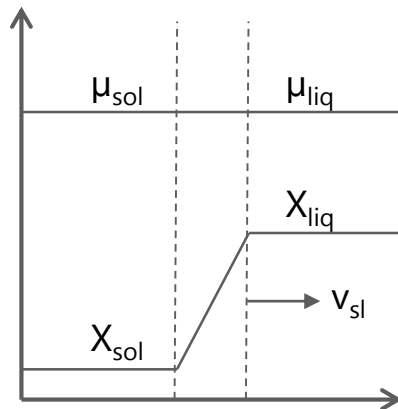


$$v_{sl} \ll \frac{D_{liq}}{\delta_{IF}}$$

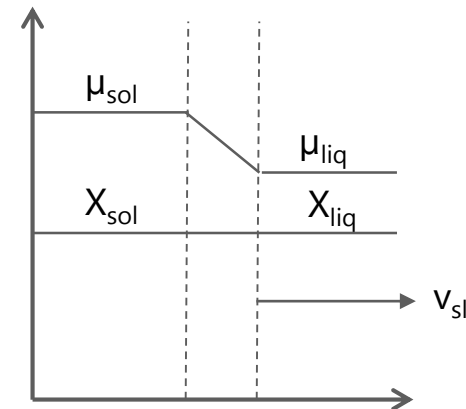
rapid cooling



$$v_{sl} \geq \frac{D_{liq}}{\delta_{IF}}$$

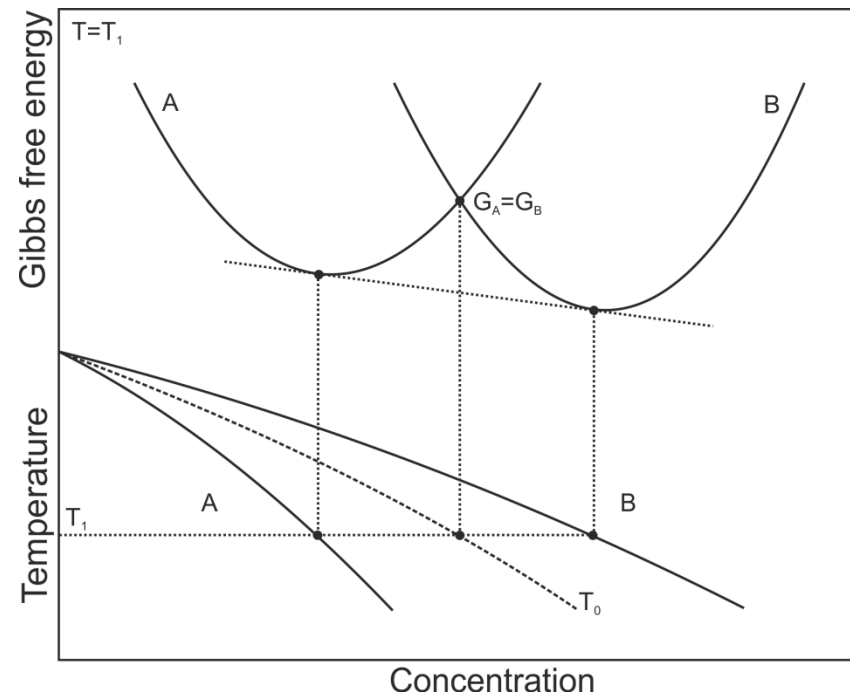


$$X_{sol} = k^m \cdot X_{liq}$$



$$X_{sol} > k^m \cdot X_{liq}$$

# Non-equilibrium phase transformations



- equilibrium phase diagram
  - common tangent construction → energy minimization by formation of two phases
  - equilibrium composition of the formed phases at  $T_1$
- diffusion-less phase transformations
  - ideally no diffusion → all phases have the same composition
  - $T$  gives the composition at which  $G_A = G_B$
  - a phase B transforms to A if  $G_A < G_B$

- Ultimate test: AM using an optimized alloy

- AM equipment
- new alloy according to specifications
- suitable powder shape

$\text{processability} = f(\text{process, powder, alloy})$

- Intermediate test: Alloy behavior during rapid melting and cooling using the AM equipment

- equipment for rapid heating and cooling (=AM equipment)
- new alloy in solid form
- no powder needed

$\llcorner \text{processability} \llcorner = f(\text{process, alloy})$

- First level test: Alloy behavior at high cooling rates

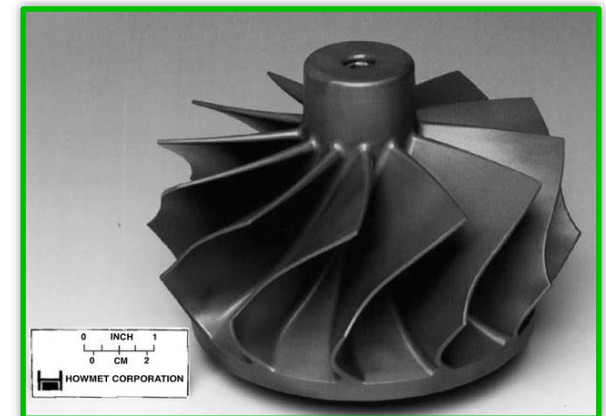
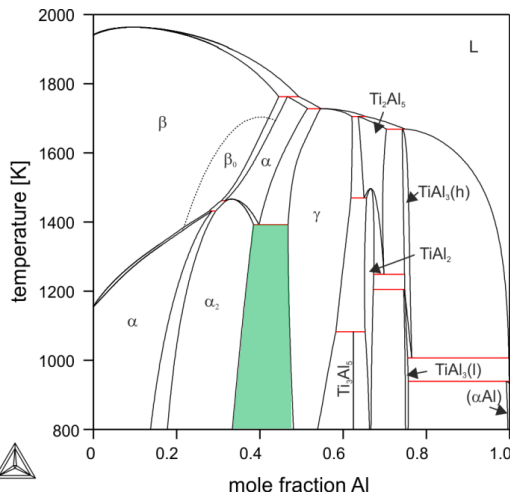
- rapid cooling equipment ( $\neq$  AM equipment)
- new alloy
- no powder needed

$\llcorner \text{processability} \llcorner = f(\text{alloy})$

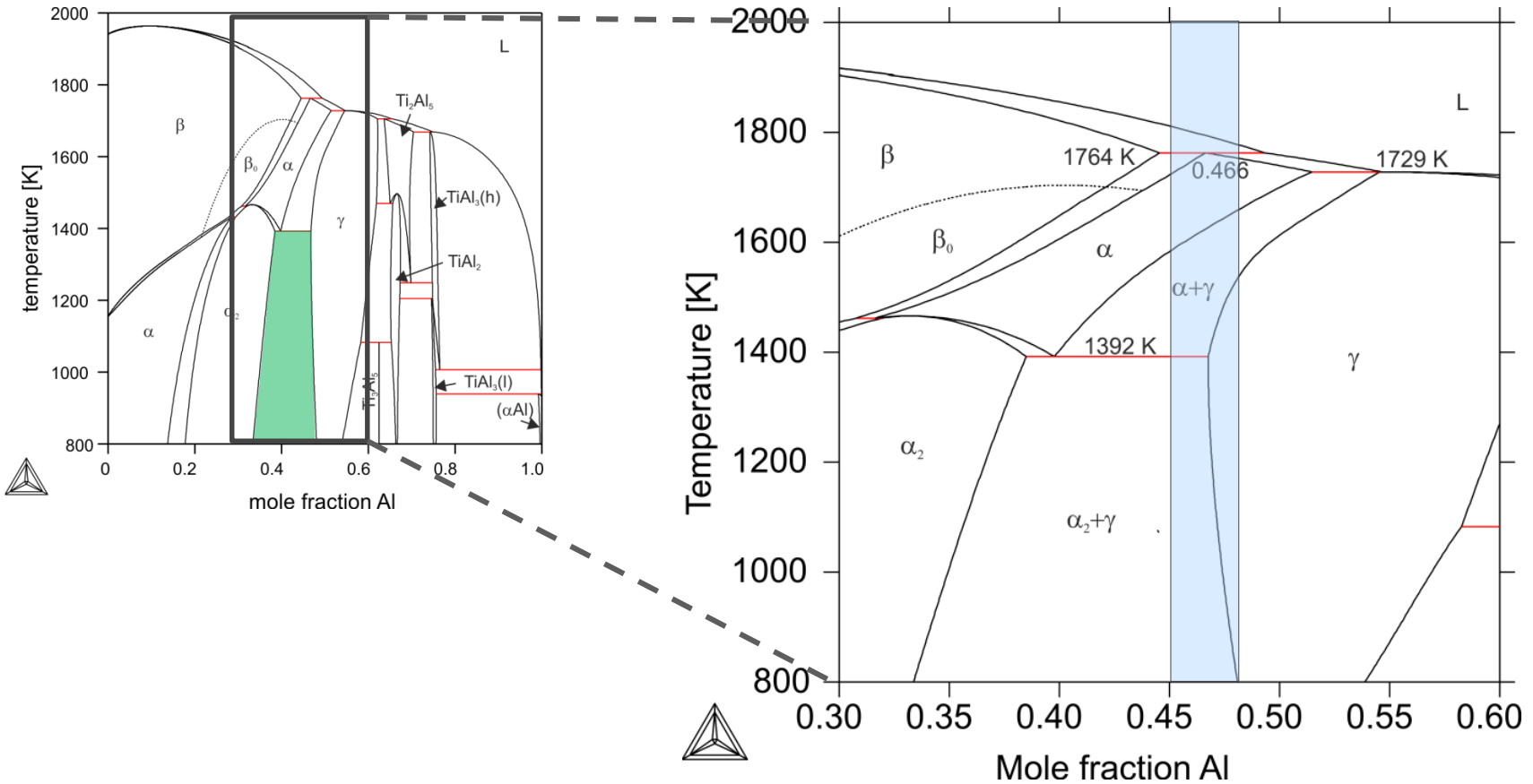
- Materials aspects related to AM – some basics
- Development of an ODS-TiAl alloy for AM
  - Microstructure formation during rapid solidification
  - Microstructure of AM processed ODS-TiAl
- Development of bronze/diamond composites for AM
  - SLM processing of bronze/diamond composites
  - Rapid solidification of Cu-Sn-Ti alloys
- Summary and outlook

# Alloy development for AM – TiAl

- Ti-Al alloys of interest for high temperature structural components
  - low density ( $\sim 3.9\text{-}4.2\text{ g/cm}^3$ )
  - high Young's modulus ( $\sim 140\text{ GPa}$ ), high strength, creep resistant
  - higher oxidation resistance than Ti alloys
  - higher service T than Ti alloys
- Fully intermetallic
  - low elongation to fracture, brittle at room temperature
  - sensitive to contamination, properties strongly dependent on phase morphology
  - Extremely difficult to process by AM

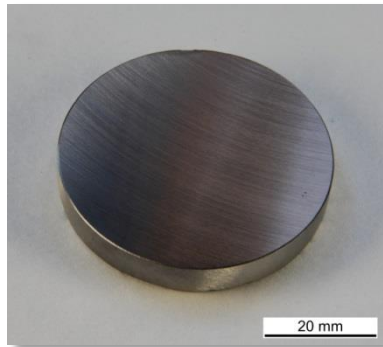


# The system Ti-Al

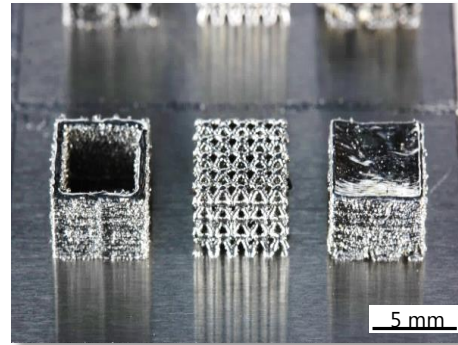


# AM of a Ti-45Al-3Nb alloy

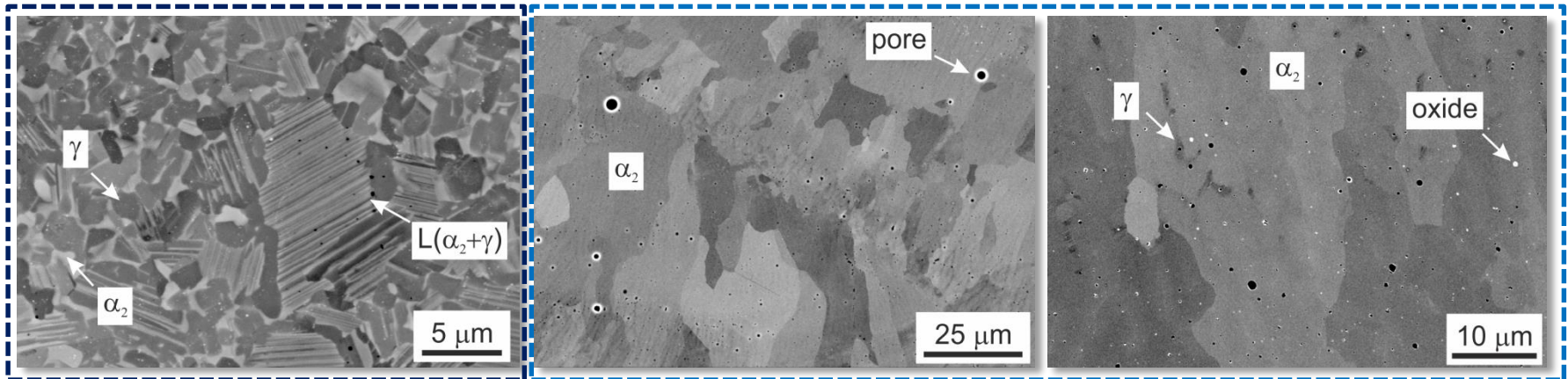
Sintering (SPS)



SLM

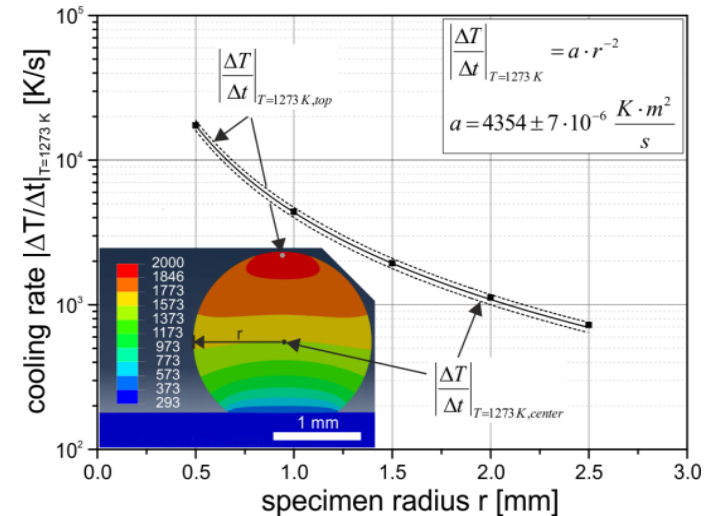
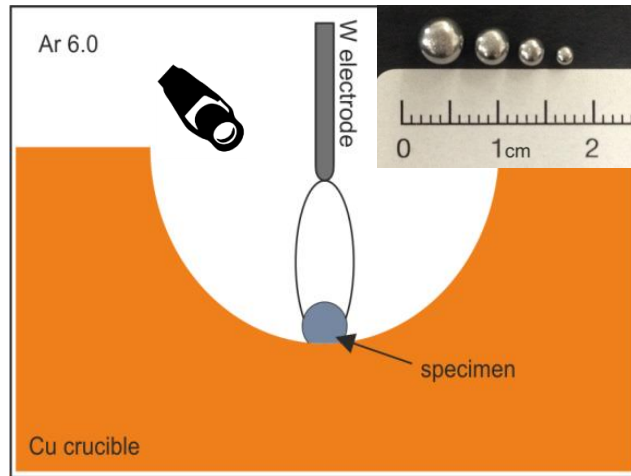


LMD



Kenel, C. *et al.*, 2016, in preparation

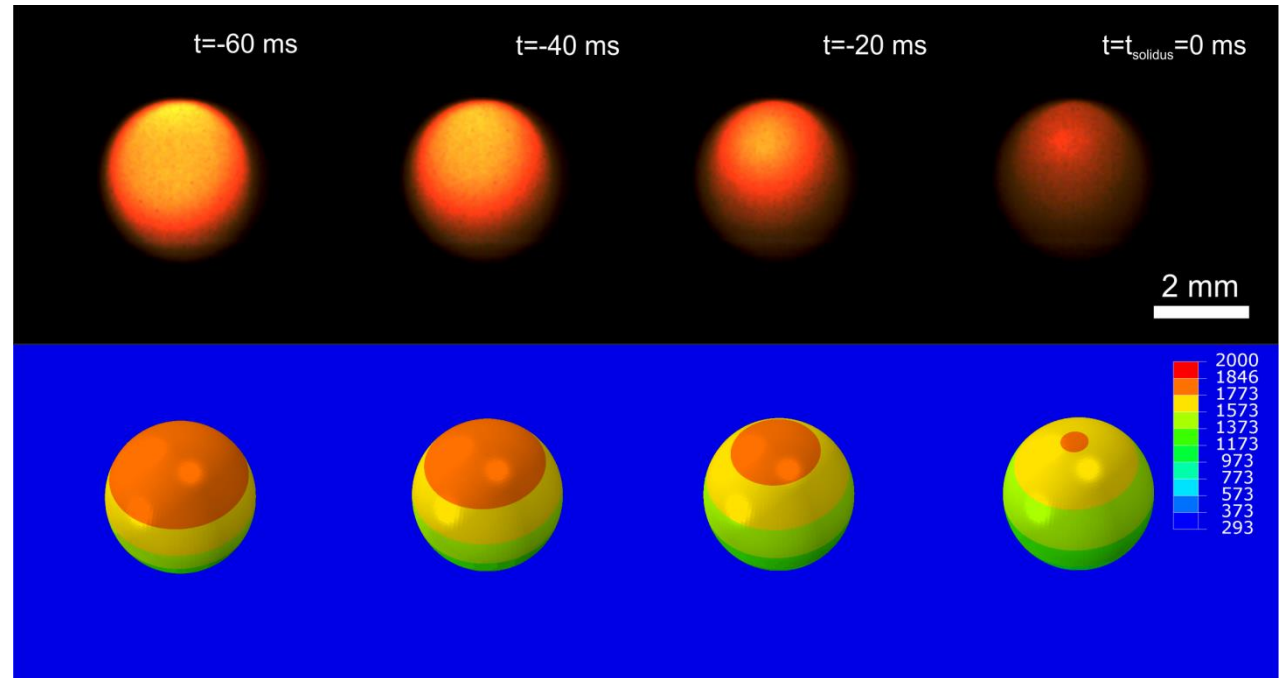
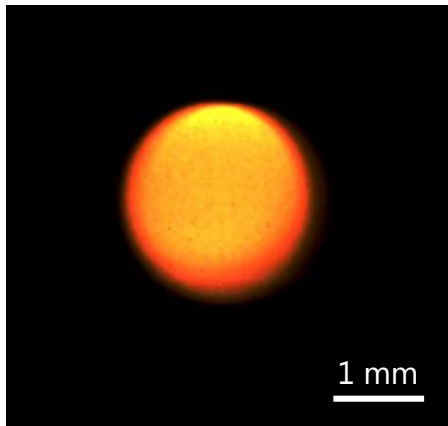
# Rapid solidification – basic offline tests



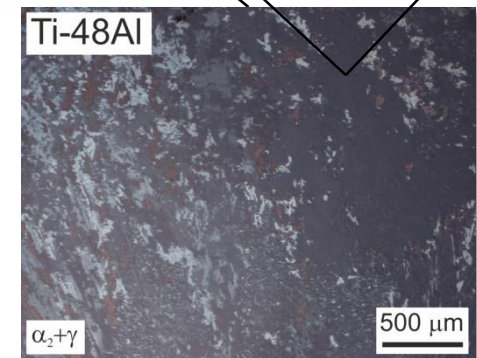
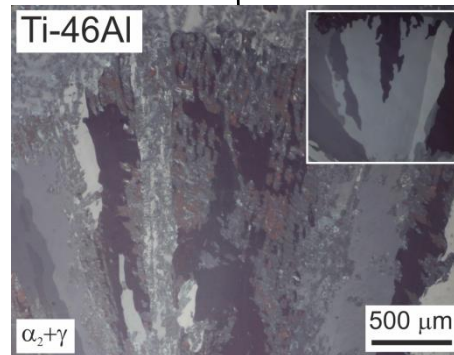
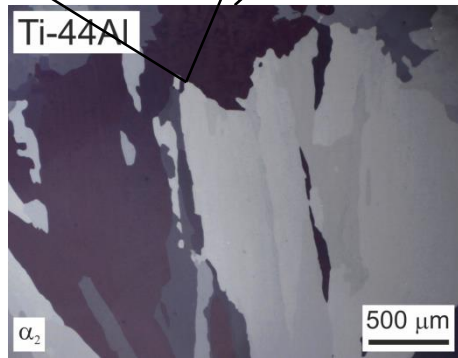
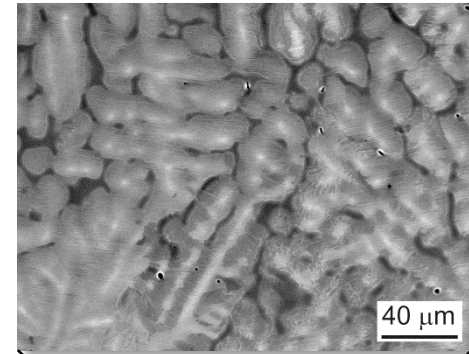
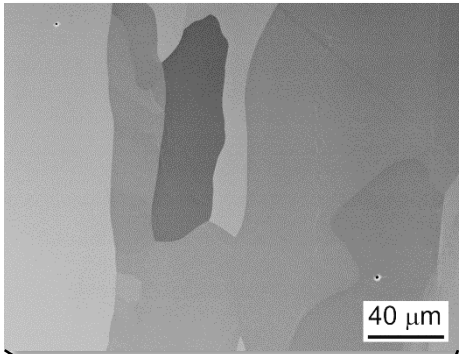
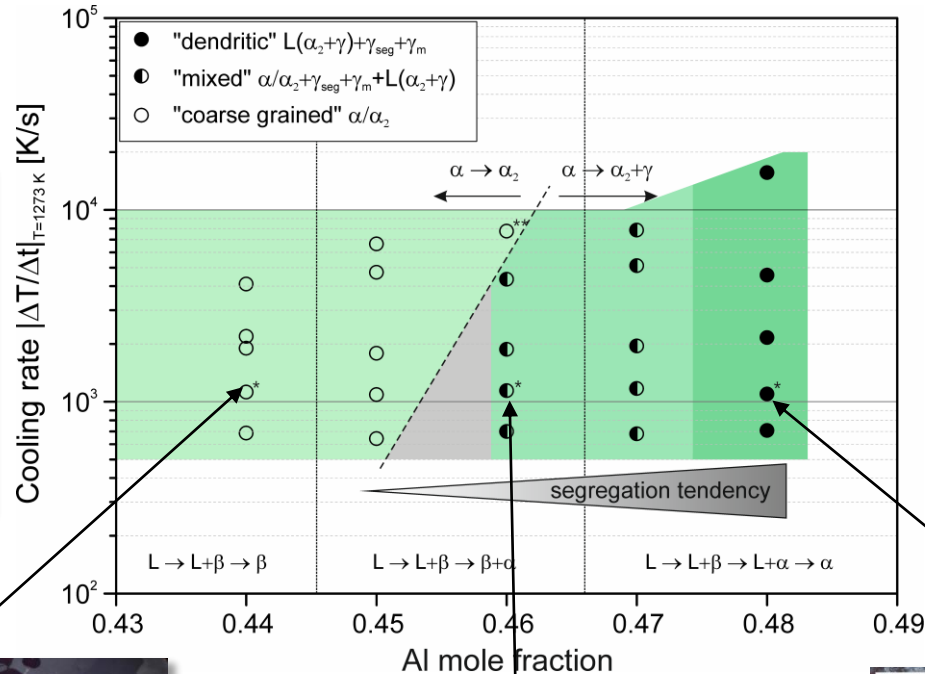
- heating and rapid solidification of small samples using W-electrode arc melting or laser beam melting
- size dependent cooling rates
  - spherical samples, the smaller the faster
  - cooling rate  $\sim r^{-2}$
- function correlating radius and cooling rate
  - single «material» parameter to describe the complete curve
- simulation verification by high speed camera measurement
  - comparable solidus propagation in experiment and simulation

/Kenel C, Leinenbach C. J Alloys Compd 2015;637:242/

# Comparison measurement - simulation

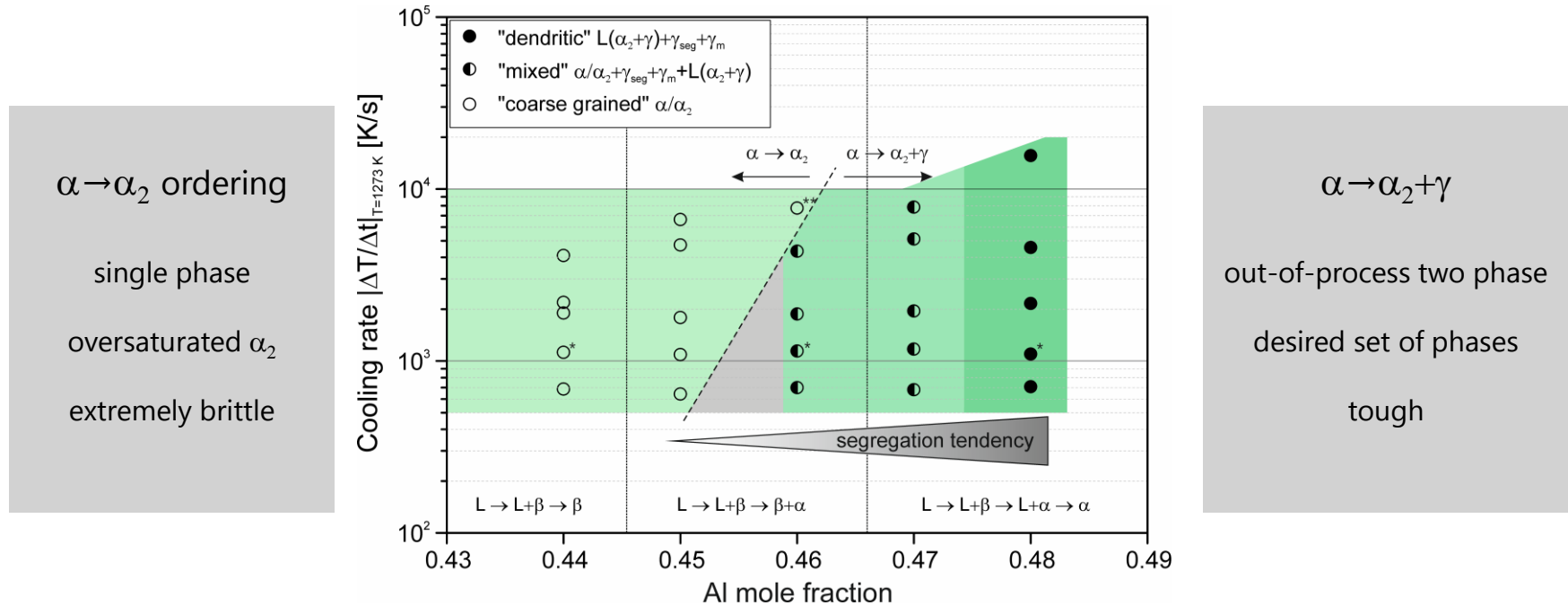


# Influence of cooling rate on microstructure formation



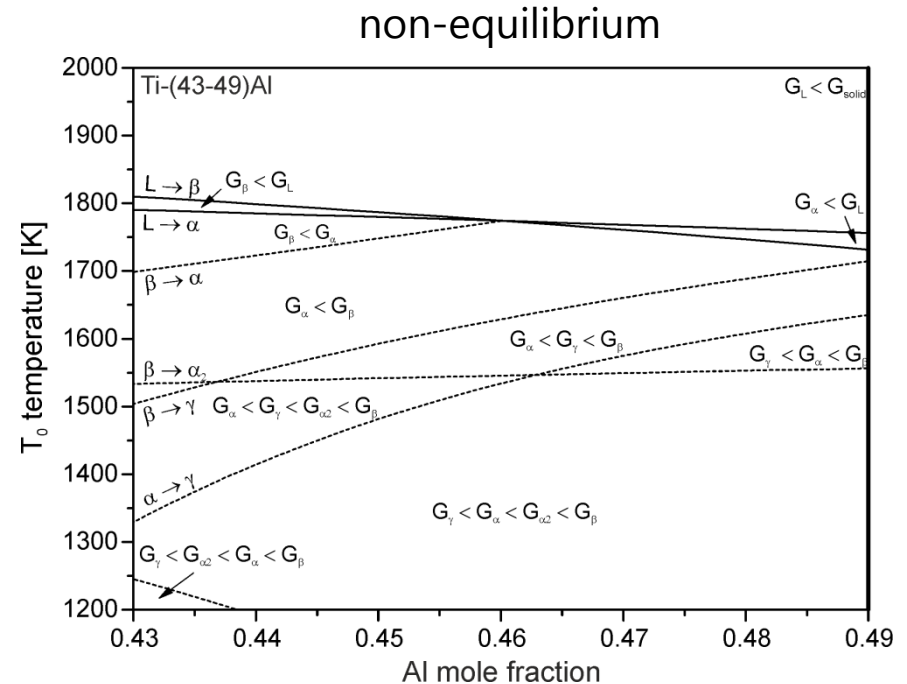
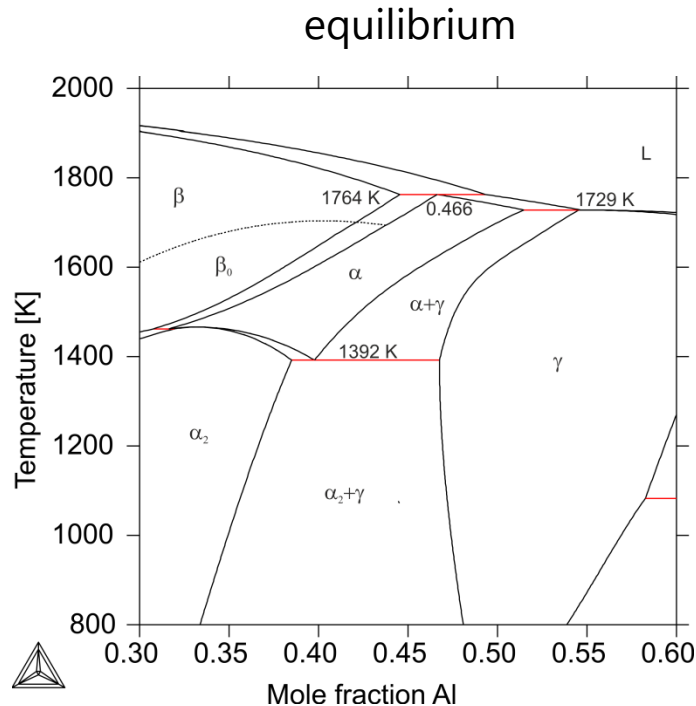
Kenel C, Leinenbach C. J Alloys Compd 2015;637:242.

# Influence of cooling rate on microstructure formation



- composition – cooling rate – microstructure maps
  - properties relevant to processing (here: formation of intermetallic phases)
  - data for alloy selection
  - similar to processing window determination experiments → indications for suitable processing parameters
- predictability based on equilibrium phase diagram information: limited

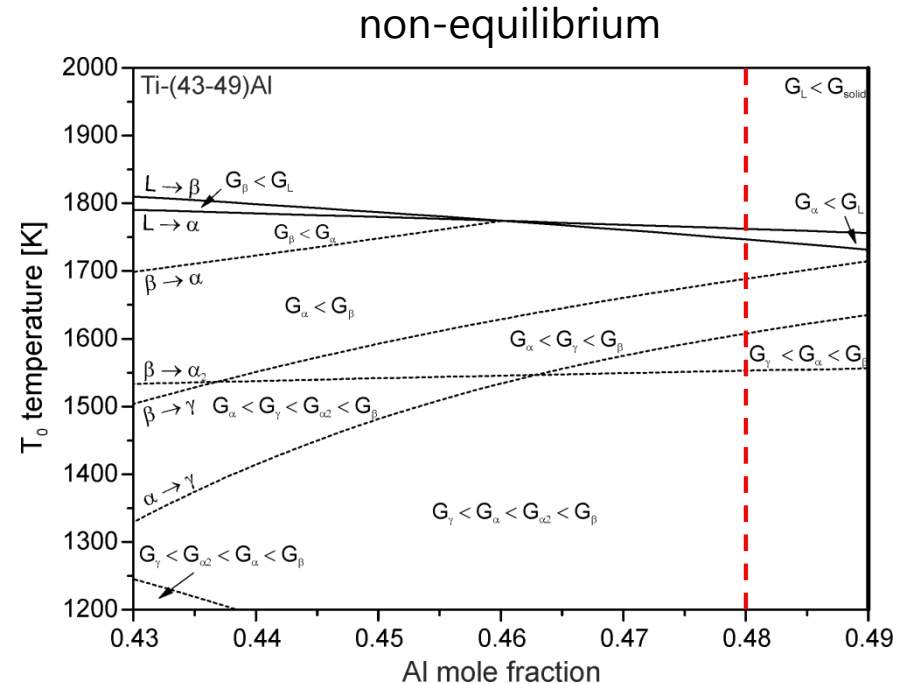
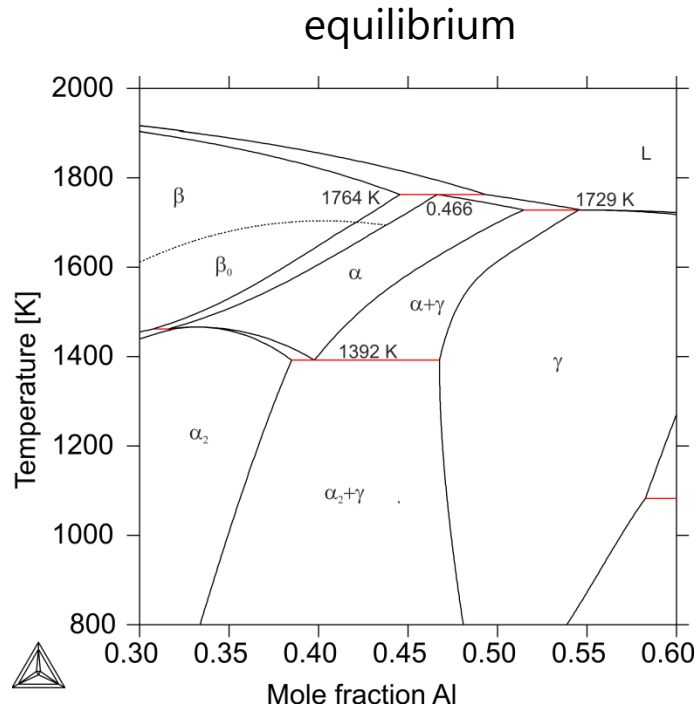
# Construction of phase selection hierarchy maps



- $T_0$  temperatures for different phase transformations and solidification
  - calculated using CALPHAD
  - based on published thermodynamic assessment for Ti-Al [VT Witusiewicz et al. J Alloys Compd 2008;465:64]
- map constituents
  - $T_0$  temperature curves for specific phase transformations
  - fields with a hierarchy according to the Gibb's free energy
- «phase diagram without diffusion»

/C. Kenel, CL. J Alloys Compd 2015;637:242/

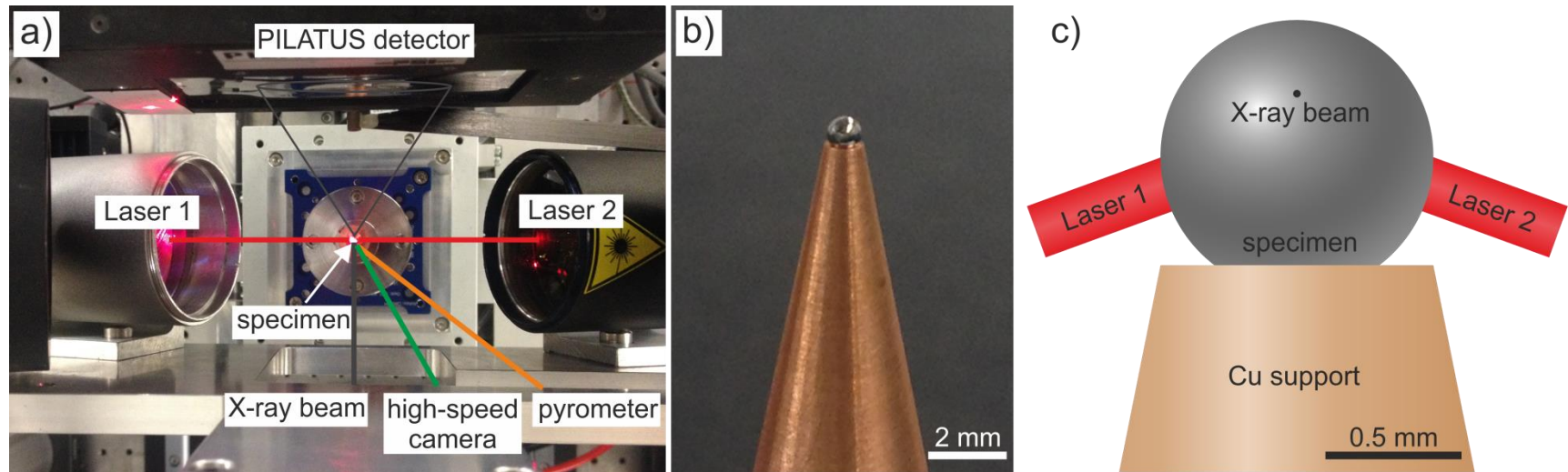
# Construction of phase selection hierarchy maps



- $T_0$  temperatures for different phase transformations and solidification
  - calculated using CALPHAD
  - based on published thermodynamic assessment for Ti-Al [VT Witusiewicz et al. J Alloys Compd 2008;465:64]
- map constituents
  - $T_0$  temperature curves for specific phase transformations
  - fields with a hierarchy according to the Gibb's free energy
- «phase diagram without diffusion»

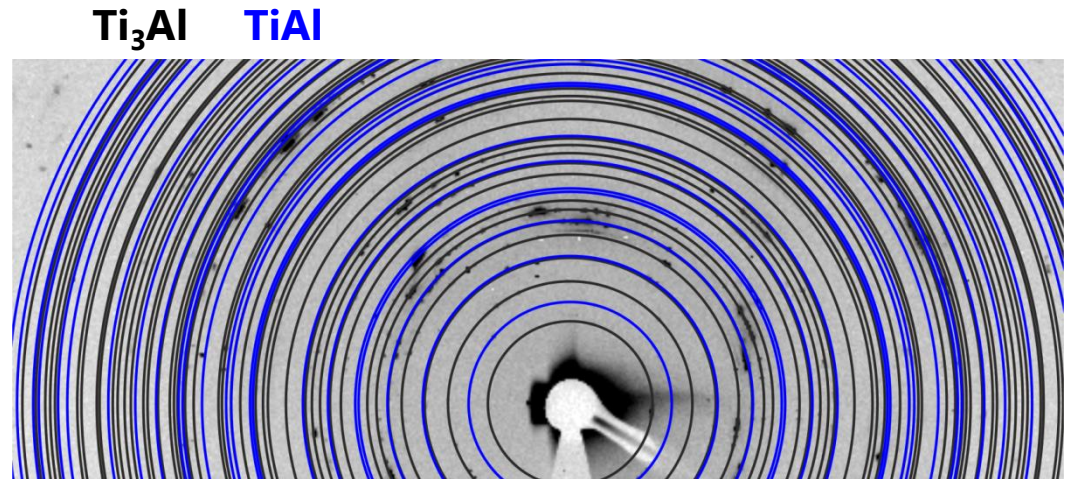
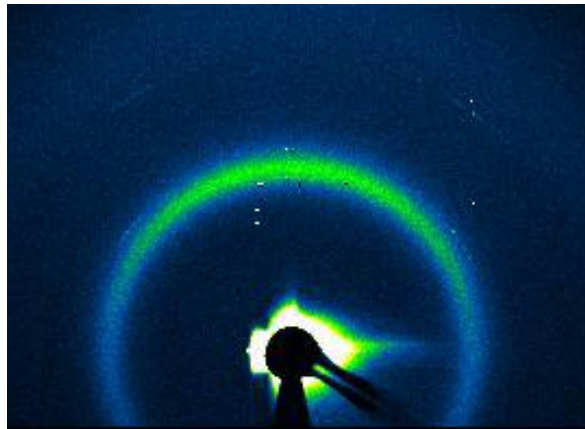
/C. Kenel, CL. J Alloys Compd 2015;637:242/

# Validation - In situ microXRD tests



- Laser heating setup in microXAS beamline at Paul-Scherrer-Institut
- Rapid melting and solidification in spherical alloy specimens; cooling rate determined by sphere radius (C. Kenel, CL. J Alloys Compd 2015;637:242)
- Time resolved characterization of phase transformations during rapid solidification using microXRD (transmission) and high speed imaging
- Study of solidification sequence in Ti-48Al at cooling rate of  $1.25 \cdot 10^3 \text{ K} \cdot \text{s}^{-1}$

# In situ microXRD tests

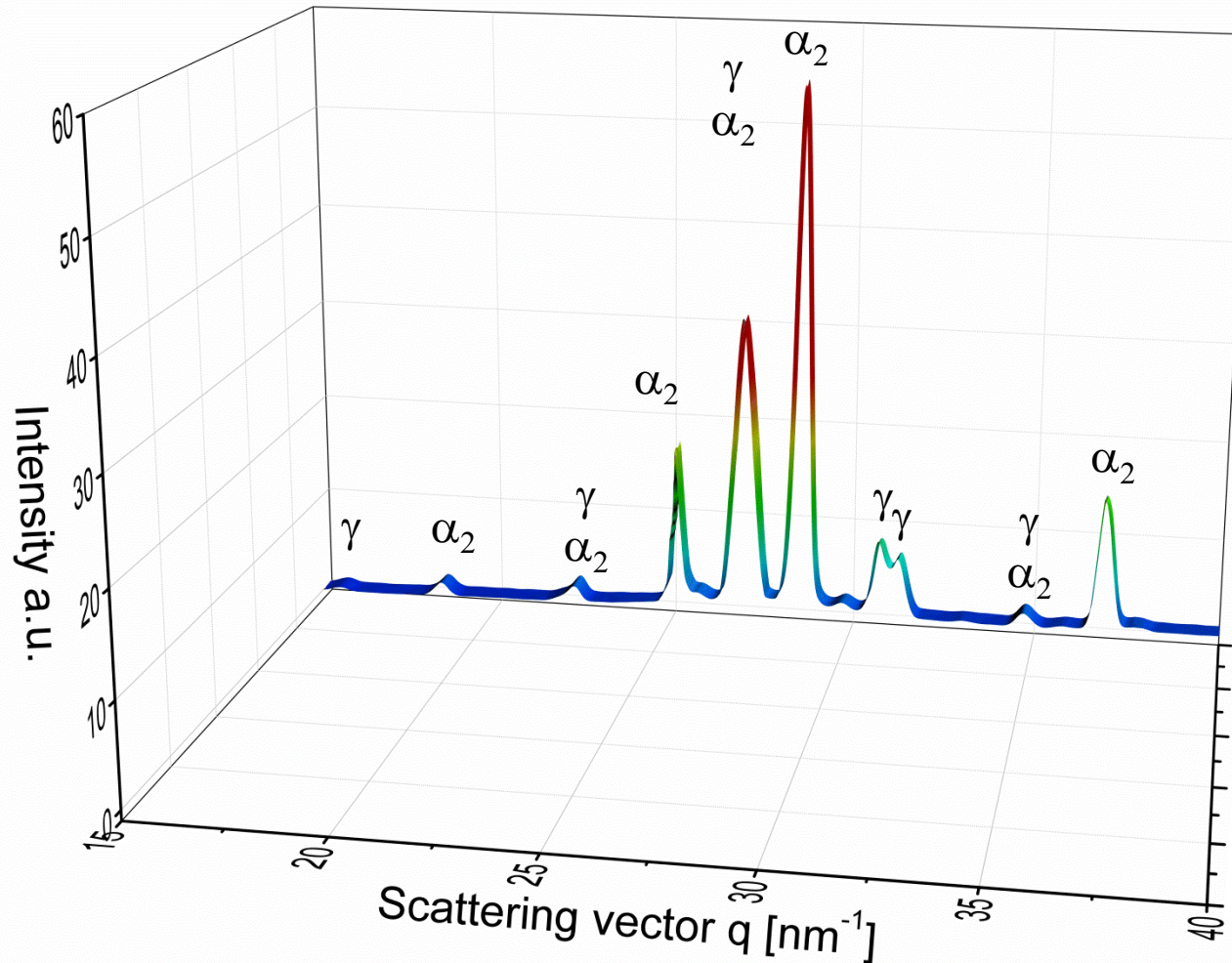


$$t_{\text{tot}} = 1.5 \text{ s}$$

- Laser heating until stable melt is reached for >1s and shut-off
- Azimuthal integration for time evolution series
- 1 Experiment = 2000 2D spectra (new measurements: 10000 2D-spectra!)

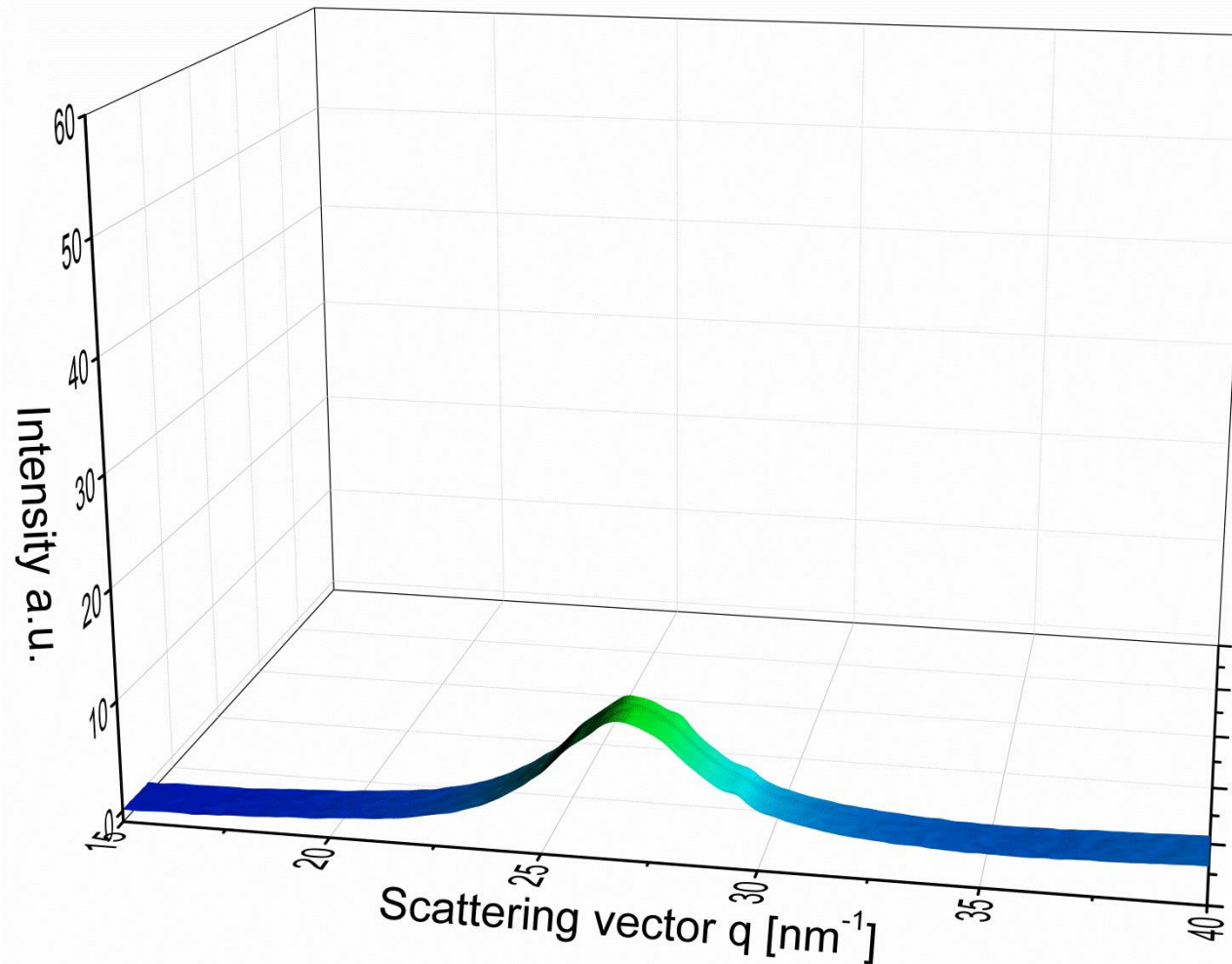
/C. Kenel, D. Grolimund, J.L. Fife, V.A. Samson,  
S. Van Petegem, H. Van Swygenhoven, CL,  
Scripta Mater 2016:114;117/

# In situ microXRD on binary Ti-48Al



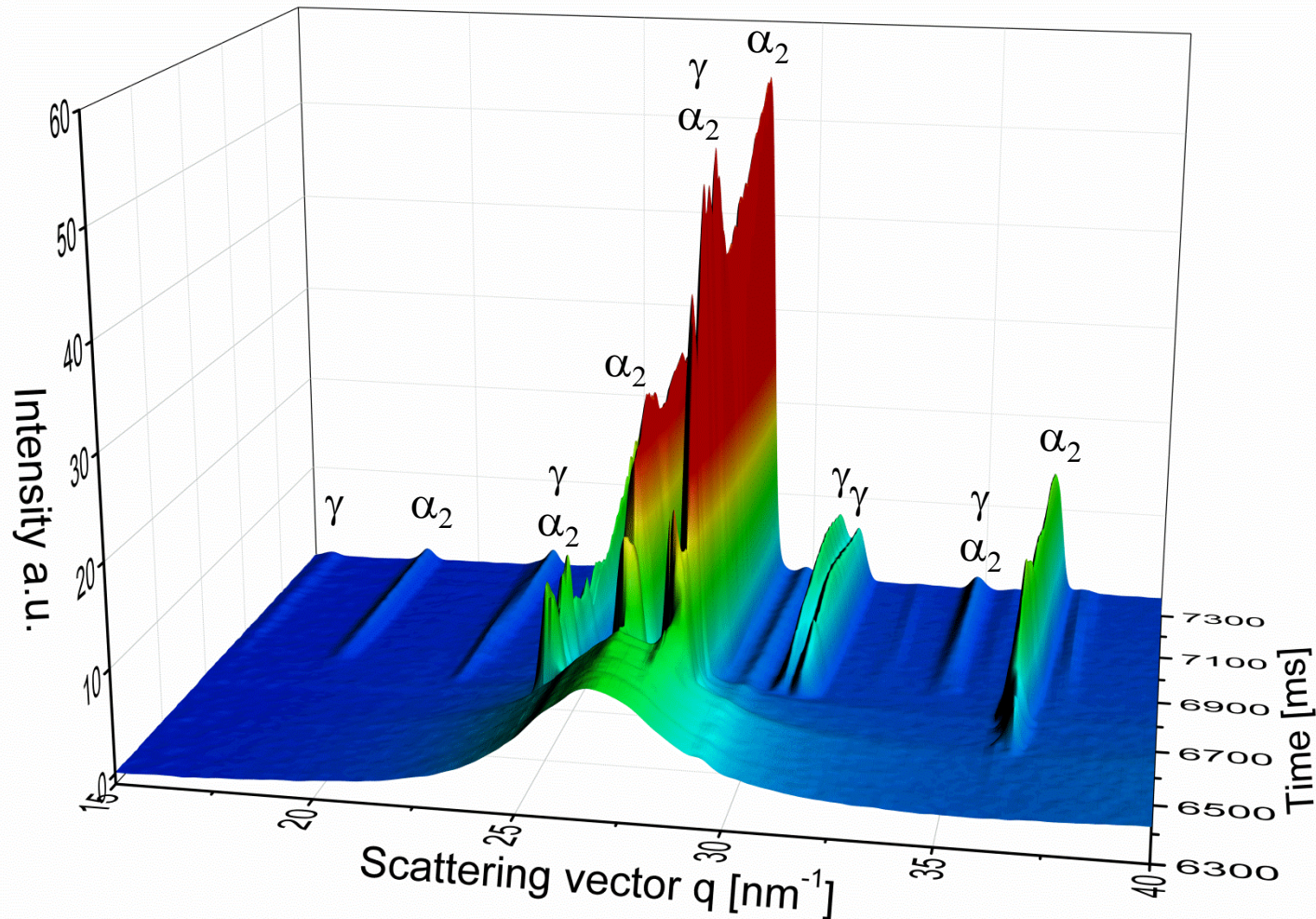
- Low T: Fully intermetallic dual phase structure

# *In situ* microXRD on binary Ti-48Al



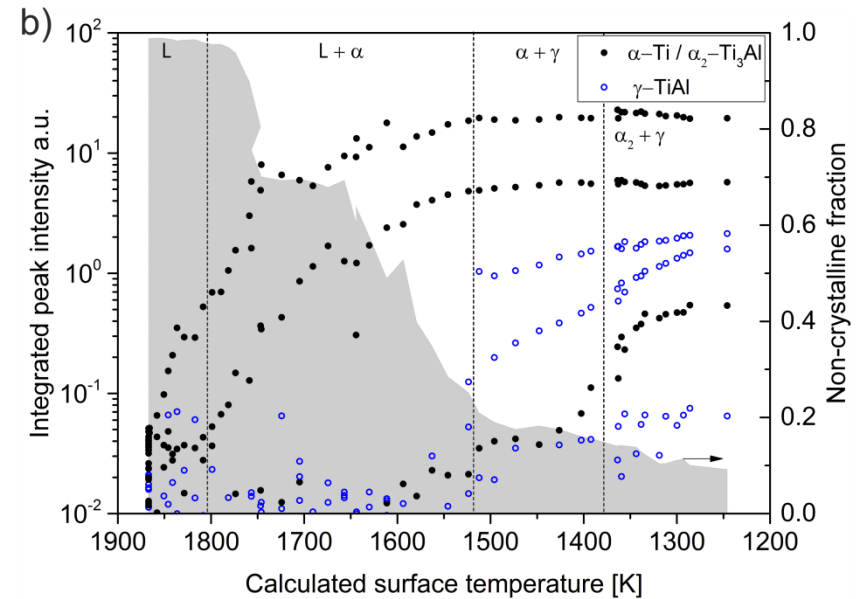
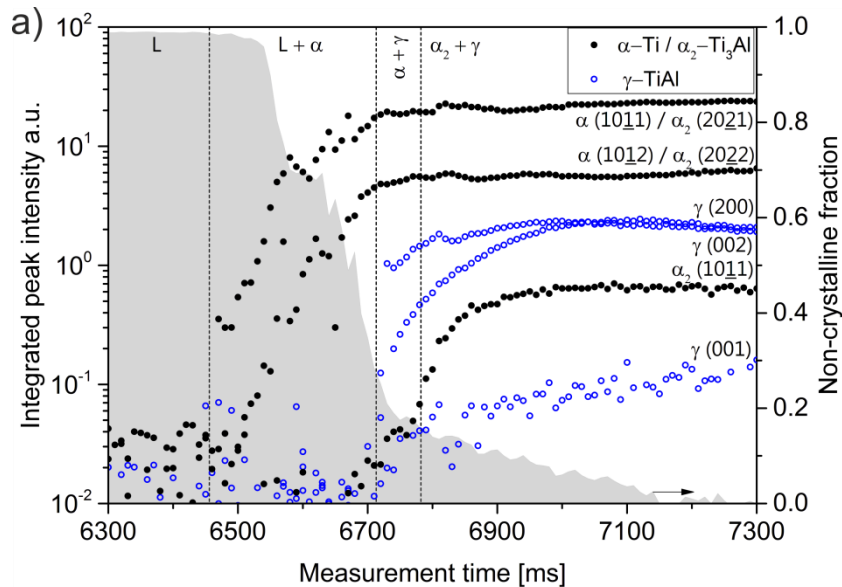
- Low T: Fully intermetallic dual phase structure
- High T ( $\sim 1500^\circ\text{C}$ ): metallic liquid

# In situ microXRD on binary Ti-48Al



- Low T: Fully intermetallic dual phase structure
- High T ( $\sim 1500^{\circ}\text{C}$ ): metallic liquid
- and everything in between....

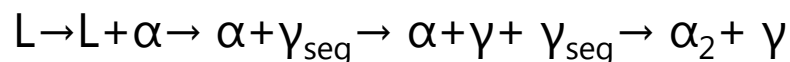
# In situ microXRD tests



- Analysis of peak evolution and non-crystalline fraction shows the coexistence of the liquid phase and the  $\alpha$ -phase upon solidification
- Pixel intensities on CCD chip can be correlated with actual surface temperature

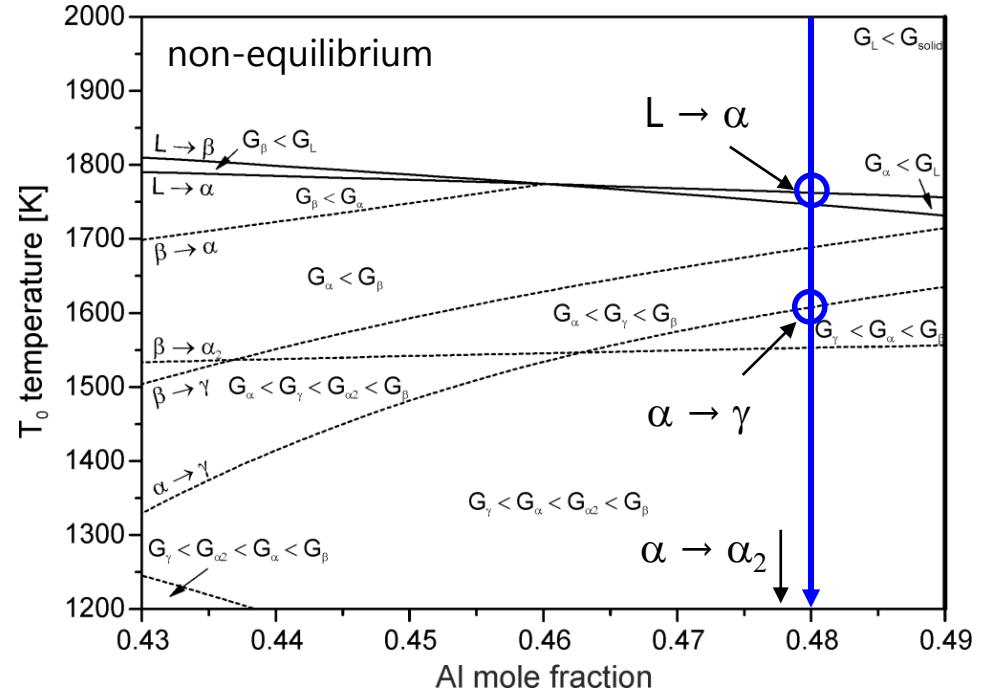
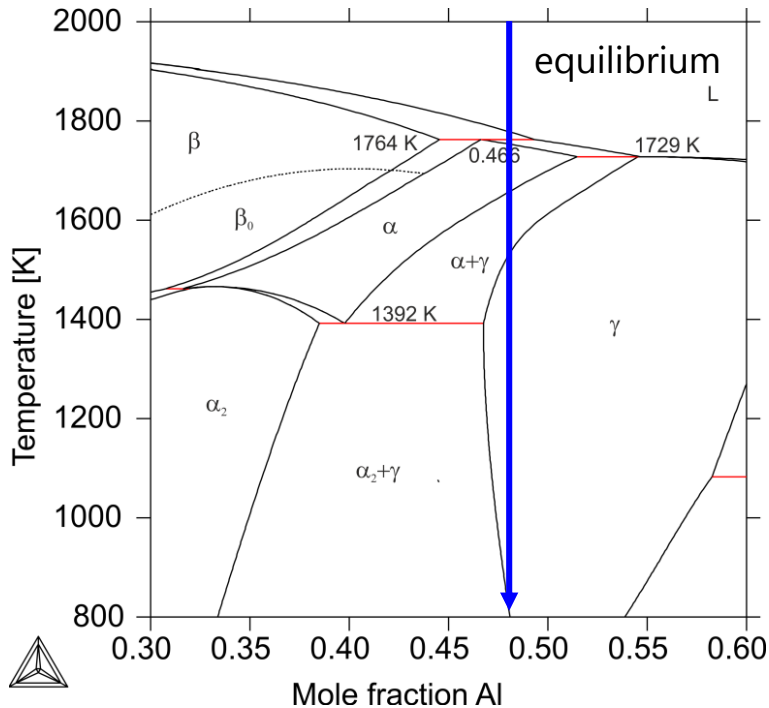
$$I_{CCD} = \frac{a \cdot c_{1L}}{\exp\left(\frac{c_2}{b \cdot T}\right) - 1}$$

- Based on the presented results, the non-equilibrium solidification and transformation of Ti-48Al follows:



/C. Kenel, D. Grolimund, J.L. Fife, V.A. Samson,  
S. Van Petegem, H. Van Swygenhoven, CL,  
Scripta Mater 2016:114;117/

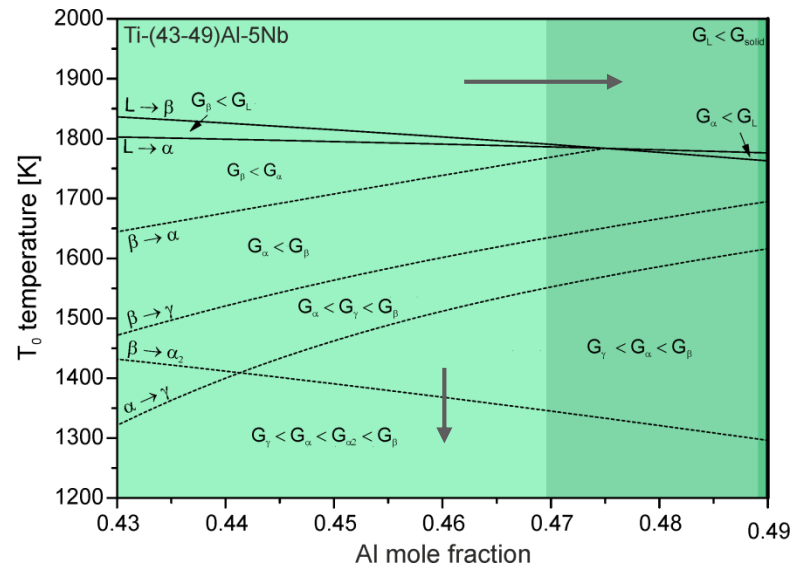
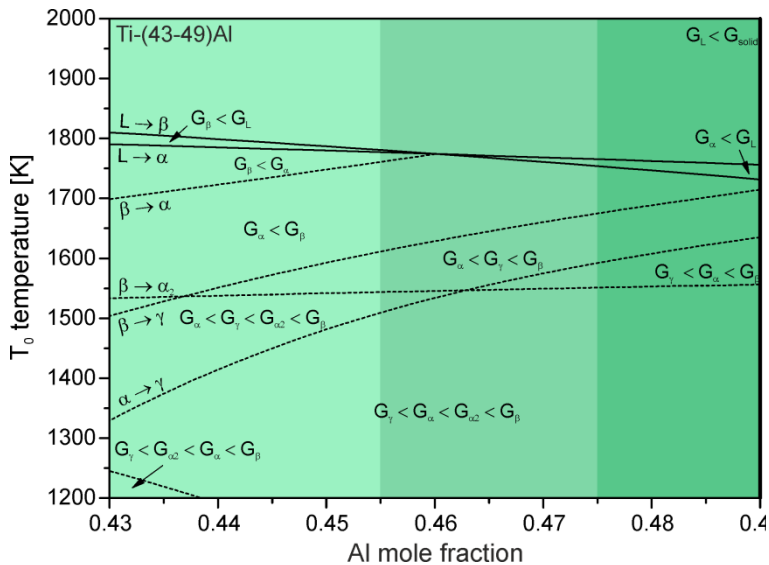
# Phase evolution under AM conditions



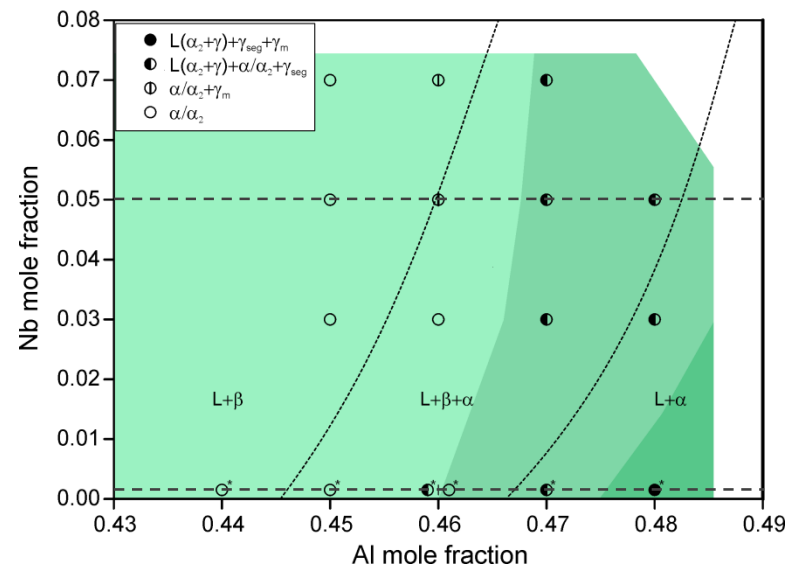
## Phase transformation sequence

- Full equilibrium:  $L \rightarrow L + \beta \rightarrow L + \beta + \alpha \rightarrow L + \alpha \rightarrow \alpha \rightarrow \alpha + \gamma \rightarrow \gamma \rightarrow \gamma + \alpha_2$
- AM conditions:  $L \rightarrow L + \alpha \rightarrow \alpha \rightarrow \alpha + \gamma \rightarrow \gamma + \alpha_2$ 
  - Preference of  $\alpha$  over  $\beta$  under non-equilibrium conditions
  - Early formation of  $\gamma$
  - Suppression of full  $\alpha \rightarrow \gamma$  transformation and direct ordering  $\alpha \rightarrow \alpha_2$

# Influence of Nb on microstructure

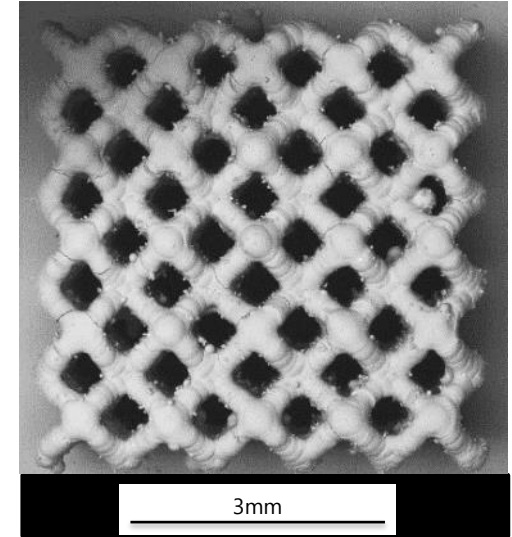
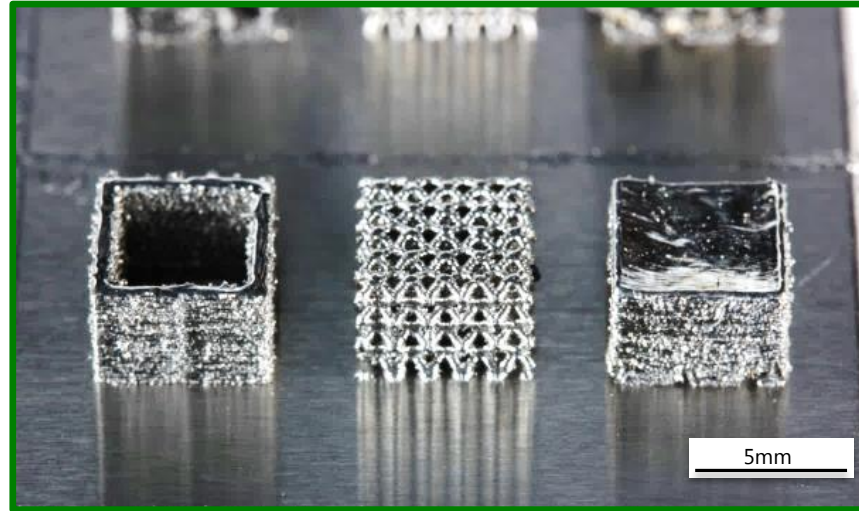
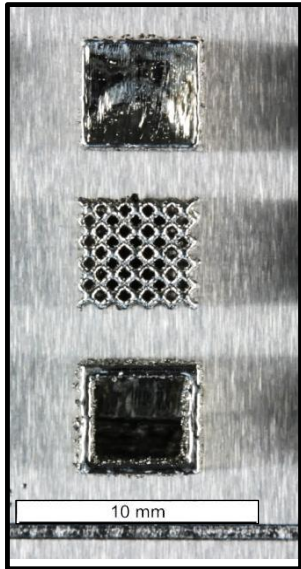


- Calculations in good agreement with experimental data
- $T_0$  concept allows to predict
  - changed transformation behavior
  - non-equilibrium effects
  - changed transformation tendencies
- if the thermodynamic assessments are available and are of sufficient quality

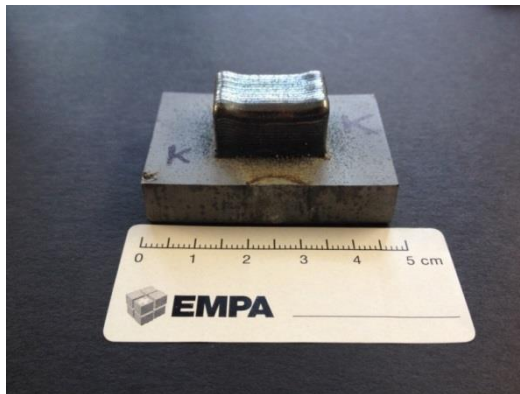


/C. Kenel, CL, Intermetallics 2016;69:82/

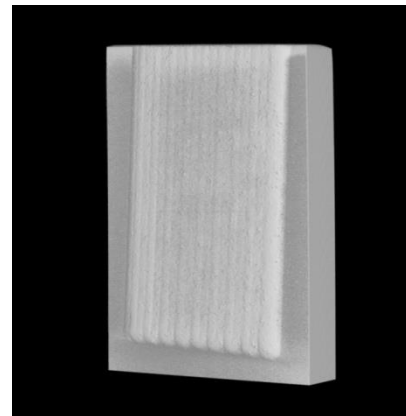
# AM of TiAl with more complex geometries



SLM 3D test structures (in collaboration with Inspire)



LMD test structure Ti-Al alloy (with TWI Ltd.)



CT of a LMD test specimen

in collaboration with  
  




- Materials aspects related to AM – some basics
- Development of an ODS-TiAl alloy for AM
  - Microstructure formation during rapid solidification
  - Microstructure of AM processed ODS-TiAl
- Development of bronze/diamond composites for AM
  - SLM processing of bronze/diamond composites
  - Rapid solidification of Cu-Sn-Ti alloys
- Summary and outlook

# New materials by AM

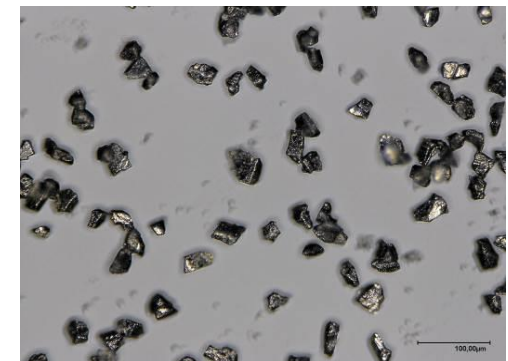
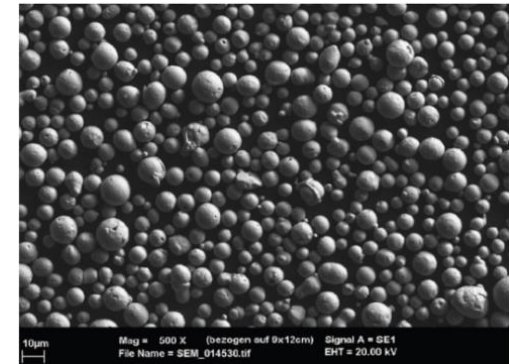
## Metal-diamond composites

- Metal-diamond composites interesting for high-performance cutting or grinding tools
- Conventional production: **Galvanic** Ni-bonding of diamond particles
  - Only single layer diamond tools possible, typically with simple geometry
- AM offers possibility to produce complexly shape geometries (e.g. internal cooling chanel)
- Problem: Graphitization tendency of diamond particles at elevated temperatures
  - Depending on atmosphere (Inert atmosphere / vacuum  $\approx 1'500^\circ$  , Air  $\approx 1'000^\circ\text{C}$ )



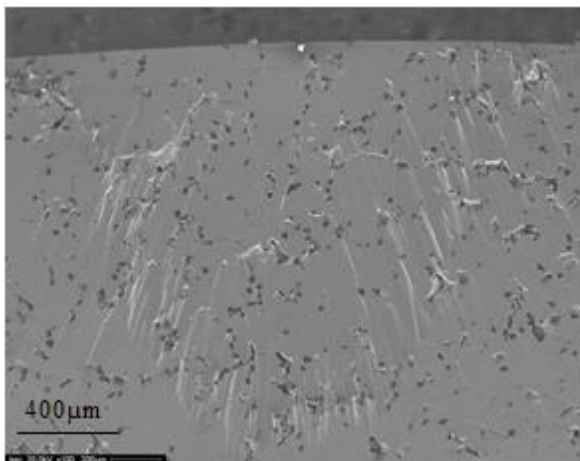
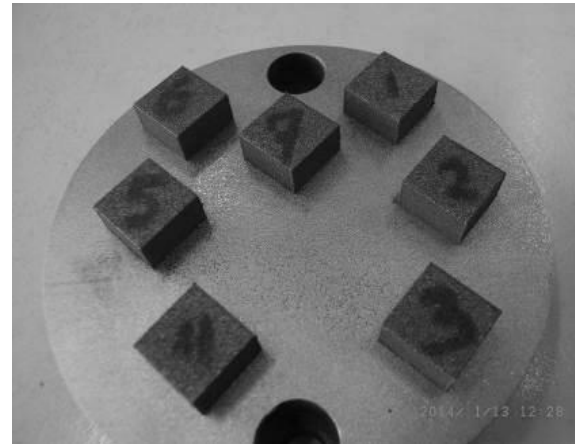
# Metal-diamond composites

- Matrix material
  - Cu-14Sn-10Ti alloy
  - High thermal conductivity ( $> \approx 55 \text{ W/mK}$ )
  - $T_{\text{liquidus}} = 925^\circ\text{C}$
  - Powder with
    - $D_{10} = 7.6\mu\text{m}$
    - $D_{50} = 20\mu\text{m}$
    - $D_{90} = 38\mu\text{m}$
  
- Diamond particles
  - 50 vol% Ni-coated to protect the diamond particles from graphitization (additional heat sink)
  - Mean particle  $\varnothing$   
 $33.9 \pm 6.4\mu\text{m}$

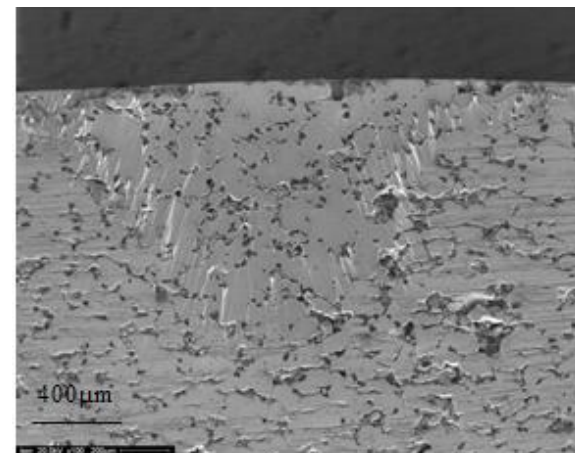


# Metal-diamond composites

- SLM processing of a of Cu-Sn-Ti alloy & diamond particles
  - Stable specimens with good surface quality can be produced



Diabrazed with 10 vol% Ni-coated diamond,  $EL = 50.5 \text{ J/mm}^3$

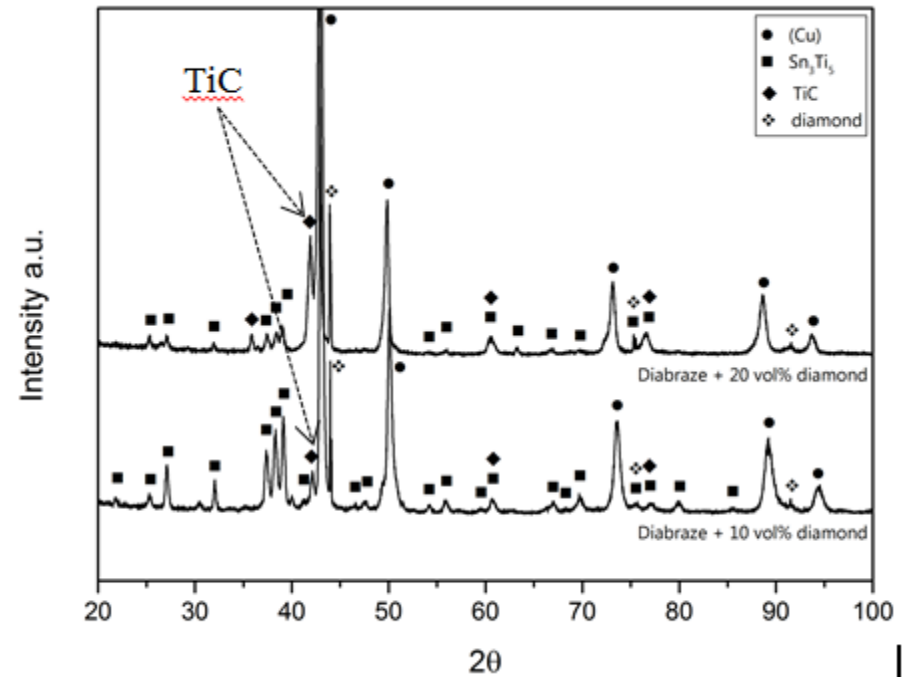
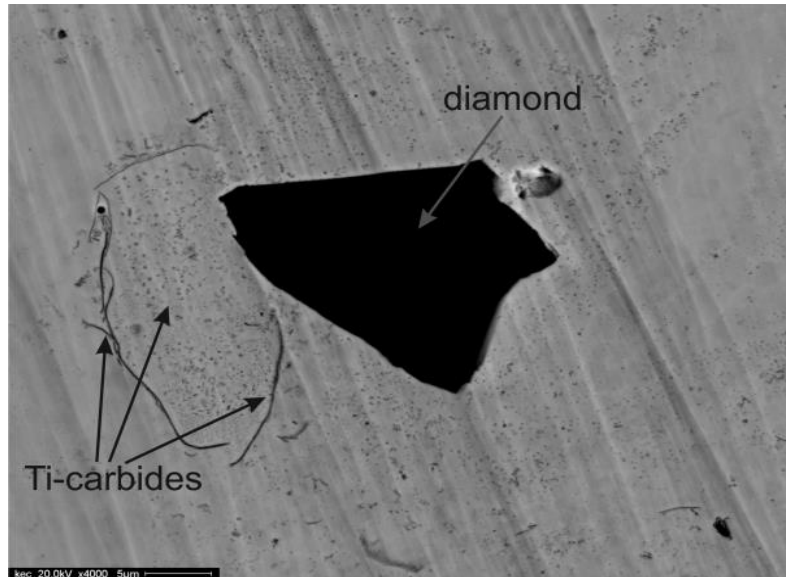


Diabrazed with 20 vol% Ni-coated diamond,  $EL = 41.2 \text{ J/mm}^3$

/A.B. Spierings, CL, C. Kenel.  
K. Wegener, Rapid Prot J,  
2016; 21(2):130-136/

# Metal-diamond composites

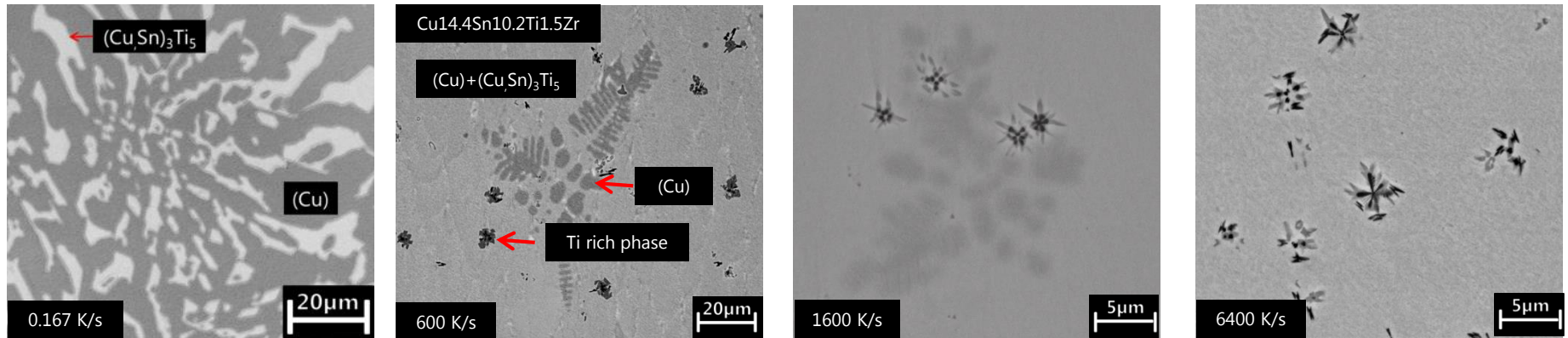
## Integrity of diamonds after SLM



- Intact diamonds, embedded in the matrix
- Diamonds are surrounded by very small TiC particles
- Diamond particles partly dissolve into the matrix during the SLM-process, forming TiC particles

/A.B. Spierings, CL, C. Kenel.  
K. Wegener, Rapid Prot J,  
2016; 21(2):130-136/

# Cooling rate dependent microstructure in Cu-Sn-Ti alloys

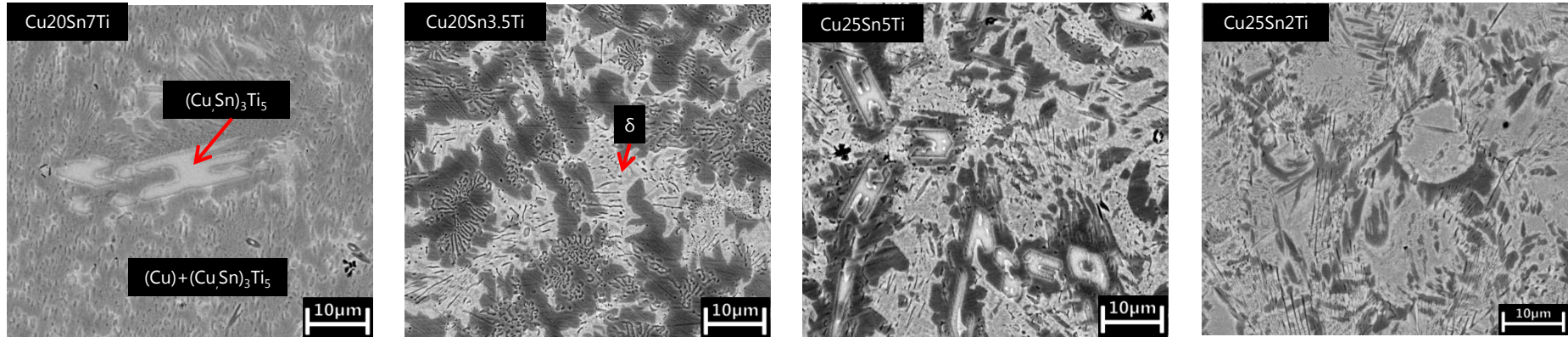


in wt.%

- Main phase constitutes (fcc (Cu) and  $(\text{Cu,Sn})_3\text{Ti}_5$ ) don't change with modification of cooling rate.
- Increasing cooling rate:
  - Grain sizes significantly decrease
  - Morphology: eutectic lamellar structures
  - Suppress of dendritic primary phase
  - Small amount of Ti enriched phases

# Composition dependent microstructure in Cu-Sn-Ti alloys

cooling rate  $\sim 600$  K/s



- Slightly changing the Ti content, the amount of large IMC is reduced.
- Different Sn/Ti ratios:
  - The phase constitutes change, i.e. new  $\delta$  phase
  - The morphology of (Cu) phase varies from dendrite to non-dendritic shape.

- Materials aspects related to AM – some basics
- Development of an ODS-TiAl alloy for AM
  - Microstructure formation during rapid solidification
  - Microstructure of AM processed ODS-TiAl
- Development of bronze/diamond composites for AM
  - SLM processing of bronze/diamond composites
  - Rapid solidification of Cu-Sn-Ti alloys
- **Summary and outlook**

- Metal additive manufacturing offers novel and hitherto unknown possibilities in terms of geometry and functionality of components
- To exploit those possibilities, the understanding and optimization of the currently existing alloys or the development of novel alloys is necessary
- It is crucial to know the phase relations in the alloys of interest as well as the phase transformation behaviour under the rapid solidification conditions during laser AM
- ...we are only at the beginning. Real additive MANUFACTURING (not prototyping) requires a better understanding of the correlation between design, materials, manufacturing process and component properties

# Acknowledgement

...the people at Empa

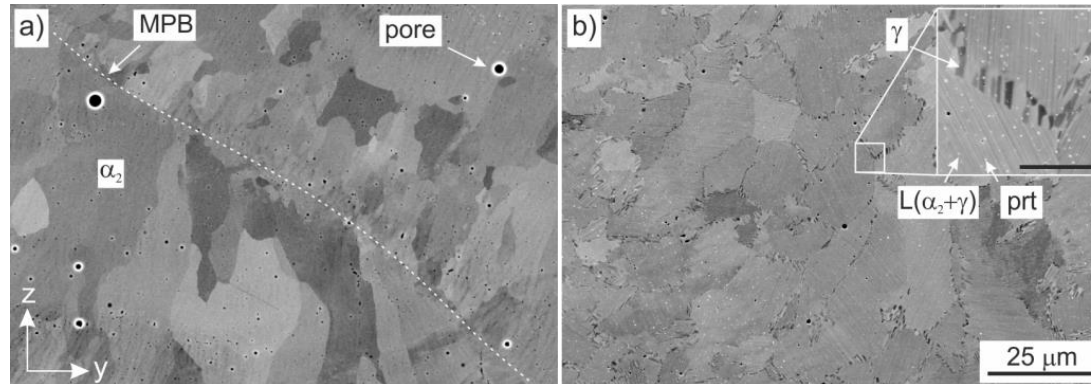
- Christoph Kenel
- Georgia Dasargyri
- Toni Ivas
- Xiaoshuan Li
- Patrik Hoffmann

...the project partners

- Thomas Bauer, inspire icams
- Adriaan Spierings, inspire icams
- Karl Dawson, ULIV
- Keith Arnold, ULIV
- Gordon Tatlock, ULIV
- Alberto Colella, MBN
- Carl Hauser, TWI
- Daniel Grolimund, PSI
- Valerie Ann Samson, PSI
- Julie L. Fife, PSI
- Steven van Petegem, PSI
- Helena van Swygenhofen, PSI

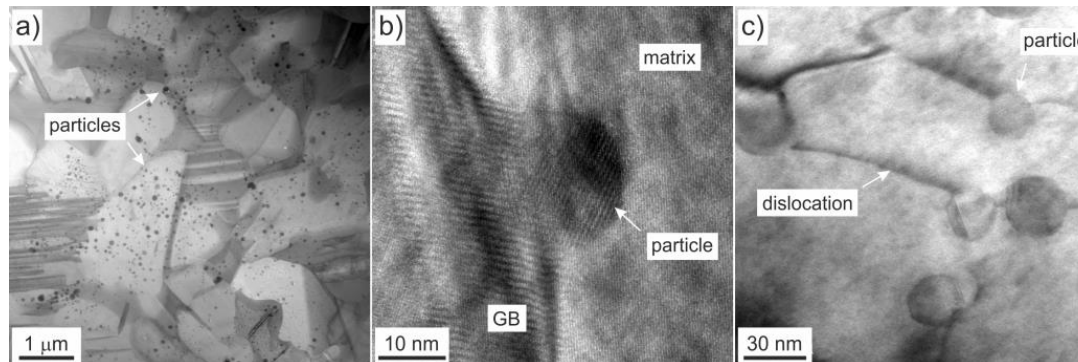
# Microstructure of AM ODS-TiAl

SEM

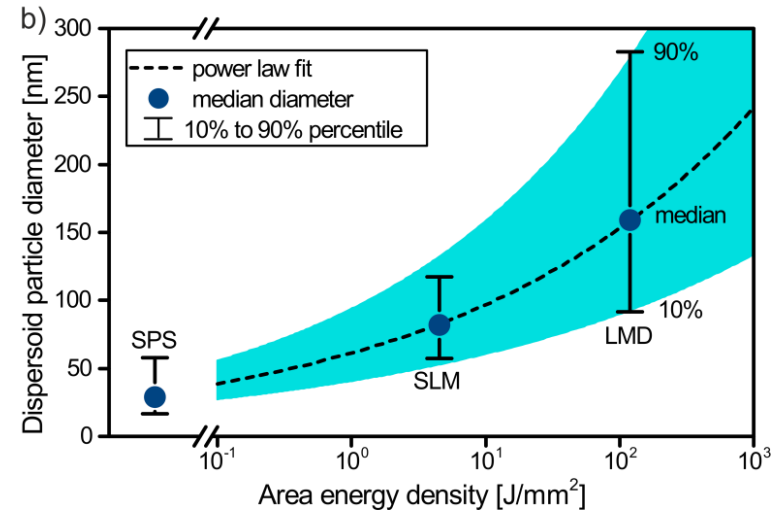
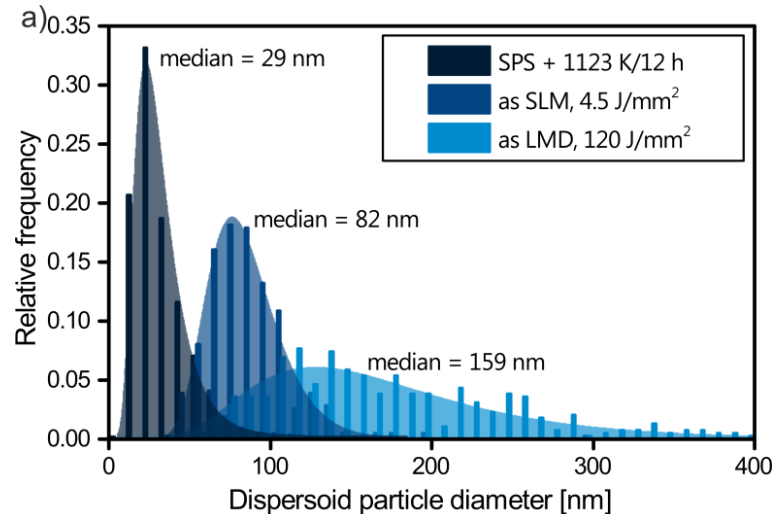


- a) as processed state → meta-stable microstructure
- b) after thermal annealing at 1123 K for 12 h (inset: scale bar = 4 μm) → ultra fine lamellar two-phase ( $\alpha_2/\gamma$ ) microstructure.

TEM



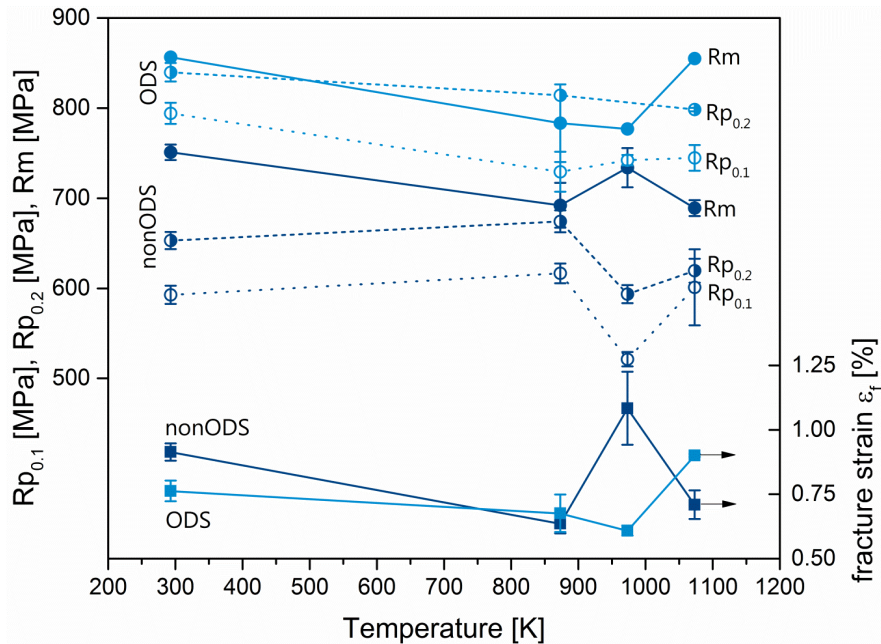
- a) STEM bright-field, distribution of fine ODS particles,
- b) HRTEM micrograph of an ODS particle pinning a grain boundary (GB) in the intermetallic matrix
- c) TEM micrograph of ODS particles interacting with dislocations.



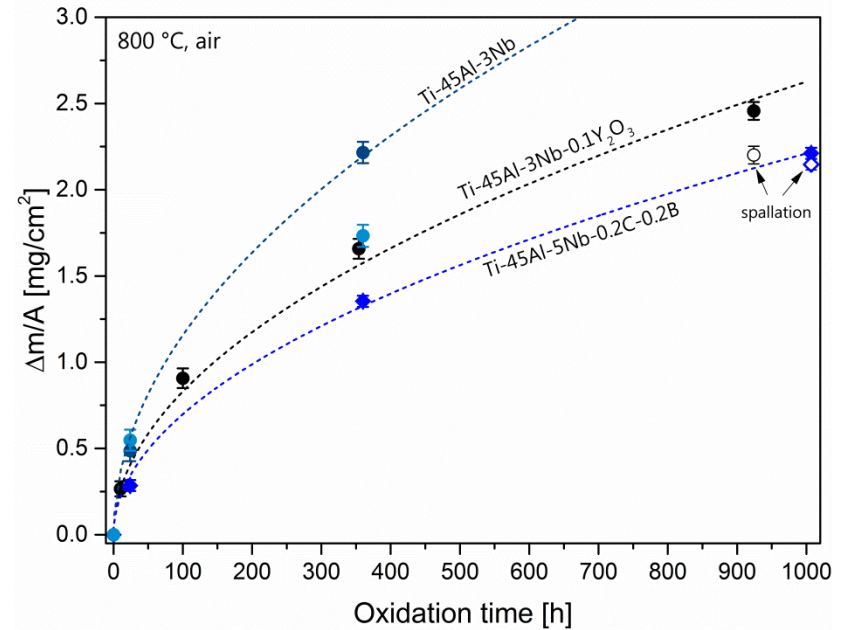
- AM processing leads to a certain degree of particle coarsening due to the high temperature and presence of a liquid phase
- Rapid growth can occur in the liquid state by incorporation of Ti and/or Al into oxides
- Reducing the energy input in the material during processing clearly reduces the preserved oxide particle size.

# Properties of ODS-TiAl

## High temperature strength



## Oxidation behavior



ODS variant has

- Higher yield point
- Higher ultimate strength
- Lower ductility



# Case 2: Ti-6Al-4V

Acta Materialia 104 (2016) 303–311

Contents lists available at ScienceDirect

Acta Materialia

journal homepage: [www.elsevier.com/locate/actamat](http://www.elsevier.com/locate/actamat)

Full length article

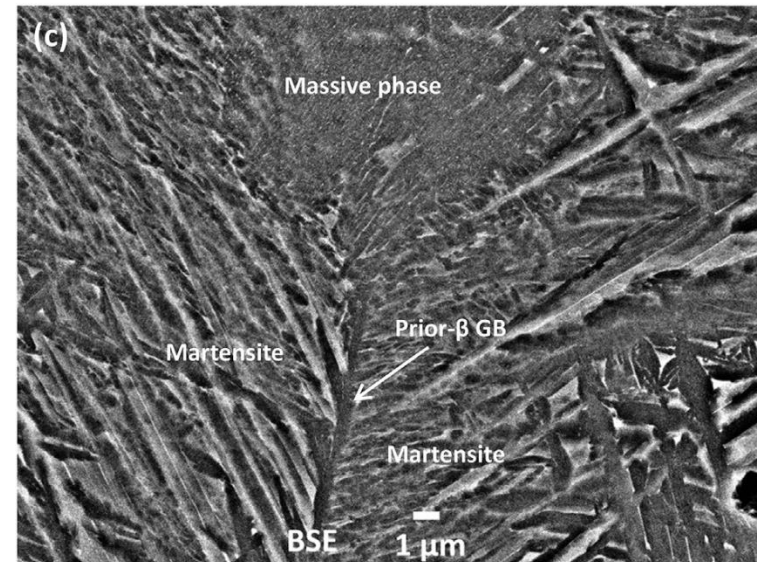
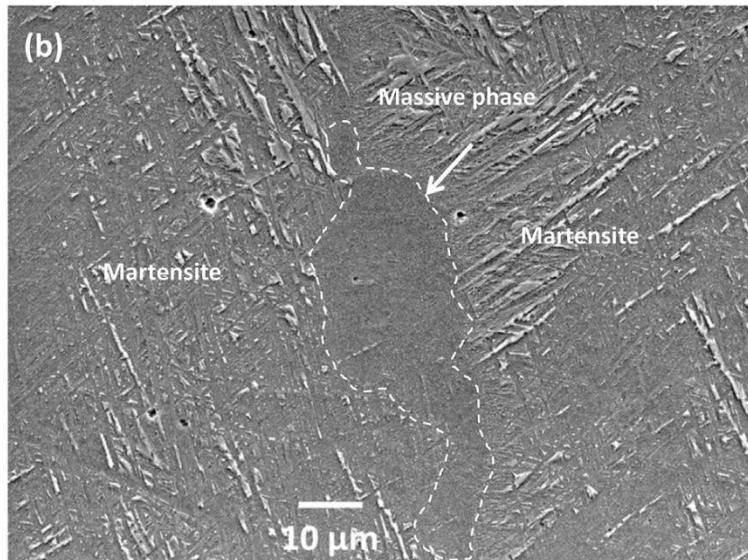
Massive transformation in Ti–6Al–4V additively manufactured by selective electron beam melting

S.L. Lu <sup>a,c,e</sup>, M. Qian <sup>b,c,\*</sup>, H.P. Tang <sup>c,\*\*</sup>, M. Yan <sup>d</sup>, J. Wang <sup>c</sup>, D.H. StJohn <sup>e</sup>

<sup>a</sup> School of Materials and Metallurgy, Northeastern University, Shenyang 110819, China  
<sup>b</sup> Centre for Additive Manufacturing, School of Aerospace, Mechanical and Manufacturing Engineering, RMIT University, Melbourne, VIC 3000, Australia  
<sup>c</sup> State Key Laboratory of Porous Metal Materials, Northwest Institute for Nonferrous Metal Research, Xi'an 710016, China  
<sup>d</sup> Department of Materials Science and Engineering, South University of Science and Technology of China (SUSTC), Shenzhen 518055, China  
<sup>e</sup> Centre for Advanced Materials Processing and Manufacturing, School of Mechanical and Mining Engineering, The University of Queensland, Brisbane, Qld 4072, Australia



- EBM processed Ti-6Al-4V
- Observation of (unusual) massive hcp- $\alpha$  grains along former bcc- $\beta$  grains in  $\alpha'$  (martensite) matrix
- Rack et al. showed that the massive transformation occurred in mill-annealed Ti-6Al-4V when cooled at cooling rates (defined at 900 C) between 20 K/s and 410 K/s.



# Case 2: Ti-6Al-4V

- Calculation of the Gibbs free energies of the hcp- $\alpha$ , bcc- $\beta$  and liquidus phase based on the TTTi3 database
- The  $\beta \rightarrow \alpha + \beta$  transus temperature is known to be 970°C
- The  $M_s$  of Ti-6Al-4V is known to be  $\approx 800^\circ\text{C}$
- The  $T_0$ -Temperature between hcp- $\alpha$  and bcc- $\beta$  is calculated to 893°C
- the cooling rates during EBM are high enough that massive  $\alpha$  grains can form in a diffusionless transformation between 893°C and 800°C
- the massive  $\alpha$  grains are not stable and decompose into  $\alpha + \beta$  lamellae as a result of the repeated re-heating during AM

